Research on Engineering Structures & Materials
www.jresm.org
Research Group

Research Article

Seismic behavior of reinforced concrete solid slab structures incorporating transfer beam systems

Mohammed. S. M. Saleh [*,1,a], Yasser R. Tawfic [1,b], L. M. Abdel-Hafez [1,c], Naglaa G. Fahmy [2,d]

[1]*Civil Engineering Department, College of Engineering, Minia University, Egypt*
[2]*Civil Engineering Department, Higher Institute for Engineering and Technology- El- Minia, College of Engineering, Nahda University, Egypt*

Article Info

Article History:

Received 05 Jan 2026

Accepted 09 June 2026

Keywords:

Transfer beams;
Floating columns;
Multi-story buildings;
Seismic analysis;
Construction sequence analysis

Abstract

This study investigates the seismic behavior of reinforced concrete multi-story buildings incorporating transfer beam systems and floating columns within solid slab configurations. The interaction between transfer beams and slabs plays a critical role in redistributing gravity and seismic loads, influencing both local demands and the global structural response. Although transfer systems are commonly used to meet architectural requirements, they introduce vertical irregularities that significantly affect seismic performance. Unlike previous studies focused on gravity loading or simplified seismic approaches, this research presents an integrated framework combining seismic analysis with Construction Stage Analysis (CSA) for reinforced concrete solid slab systems with transfer beams. A systematic parametric investigation is conducted, examining the effects of beam dimensions, continuity, location, and basement inclusion. A comprehensive numerical analysis is performed using ETABS Ultimate 22.0 for a twelve-story building designed in accordance with the Egyptian Code (ECP 203-2020), utilizing the Egyptian response spectrum for dynamic analysis. The structure is modeled with a concrete compressive strength of 30 MPa and reinforcing steel yield strength of 350 MPa. Equivalent Static Analysis (ESA), Response Spectrum Analysis (RSA), and CSA are employed to evaluate structural performance. Results indicate that CSA provides a more realistic and conservative assessment, with increases of up to 34.77% in bending moments and 28.85% in shear forces compared to RSA. Increasing transfer beam depth significantly reduces deflections by up to 82.79%, while increasing internal force demands. Beam location is critical, where perimeter placement enhances load transfer efficiency, whereas intermediate positions increase lateral displacement by up to 29.44%.

1. Introduction

Transfer systems have become an essential component in the structural design of modern multi-story reinforced concrete buildings, particularly when architectural or functional requirements impose discontinuities in vertical load-resisting elements. These systems, commonly implemented through transfer beams, deep girders, transfer slabs, or integrated transfer frames, enable the redistribution of loads from upper-story columns to alternative supporting elements at lower levels, thereby allowing greater architectural flexibility in podium structures, mixed-use developments, and buildings incorporating open parking or commercial spaces at lower floors [1-3]. The selection and placement of transfer systems are typically governed by architectural constraints, mechanical system arrangements, and construction efficiency considerations [4].

*Corresponding author: eng.mohamed.s.1992@gmail.com
[a]orcid.org/0000-0003-4418-8191; [b]orcid.org/0000-0001-6526-8727; [c]orcid.org/ 0009-0000-6921-5630; [d]orcid.org/0000-0002-7408-8506
DOI: http://dx.doi.org/10.17515/resm2026-1452st0105rs

Recent destructive earthquakes, particularly the 2023 Kahramanmaraş earthquakes in Türkiye, have highlighted the vulnerability of buildings containing vertical irregularities such as floating columns and transfer systems [5, 6]. Field observations from these seismic events demonstrate that discontinuities in vertical load paths can significantly amplify seismic demands and lead to severe damage concentration and potential progressive collapse when not properly addressed in design. Consequently, understanding the seismic behavior of structures incorporating transfer systems has become a critical issue in modern earthquake engineering.

Transfer beams are heavily reinforced structural members designed to support concentrated loads from upper-story columns and redistribute them to supporting elements below. Due to the high shear forces and complex stress distributions associated with such loading conditions, transfer beams typically behave as discontinuity regions (D-regions), where classical beam theory becomes inadequate for representing the actual stress flow within the structural element. Therefore, advanced analytical approaches such as nonlinear finite element analysis and strut-and-tie modeling are often employed to capture the complex load transfer mechanisms and shear-compression behavior occurring in these elements [7–9]. Previous studies have also examined the structural efficiency of different transfer girder systems, including conventional reinforced and prestressed configurations, highlighting their influence on load redistribution and overall structural performance [10]. In multi-story buildings incorporating floating columns, the continuity of vertical load paths is intentionally interrupted, requiring the transfer of loads through horizontal structural elements. Although such structural configurations may perform satisfactorily under gravity loads, they introduce significant irregularities in both stiffness and strength distributions that can adversely influence the seismic performance of the structure. Previous studies have reported that floating column systems may increase structural flexibility and lead to higher lateral displacements and inter-story drifts under earthquake loading conditions [11,12]. Therefore, understanding the interaction between floating columns, transfer beams, and surrounding structural components is essential for achieving reliable seismic performance in reinforced concrete buildings.

In many reinforced concrete structures, transfer beams are integrated with solid slab floor systems, forming a composite structural mechanism that significantly influences both local and global structural behavior. The interaction between slabs and beams contributes to stiffness distribution and load transfer mechanisms within the structural system. However, the influence of solid slab systems on the seismic response of buildings incorporating transfer beams has received limited attention in previous research. In particular, the interaction between transfer beams and solid slabs may significantly affect load redistribution, internal force development, and deformation behavior at the transfer level under seismic loading conditions [4,13]. Previous research on transfer systems has primarily focused on gravity load behavior or simplified static analysis approaches. Although several studies have investigated the seismic response of buildings incorporating transfer elements, many of these studies neglect the influence of construction sequence effects and time-dependent phenomena such as creep and shrinkage [14]. Construction Stage Analysis (CSA) has emerged as an advanced analytical technique capable of capturing the progressive development of stresses and deformations during the construction process by modeling the sequential addition of structural elements and loads [15,16]. Recent studies have further emphasized the importance of construction stage analysis in evaluating transfer beam behavior. For instance, Sadouki and Djafar-Henni [17] demonstrated that staged construction significantly influences the internal force distribution in transfer elements. Similarly, Mitra et al. [18] highlighted the critical role of transfer beams in enhancing seismic resilience and structural integrity in reinforced concrete buildings.

Recent analytical studies have demonstrated that neglecting construction sequencing may lead to significant underestimation of internal forces and structural deformations in reinforced concrete buildings. For instance, Construction Stage Analysis (CSA) has been shown to produce substantially higher structural demands compared with conventional static or response spectrum analyses. Research on setback steel buildings reported that story displacements may increase by up to 56%, while column axial forces can rise by approximately 48% when CSA is adopted instead of Response Spectrum Analysis (RSA) [19]. Furthermore, additional studies have confirmed the critical role of CSA in transfer beam assessment, revealing that transfer beams experience significantly higher bending moments and axial forces due to the progressive accumulation of stresses during sequential floor construction [14]. Despite these findings, only limited research has investigated the combined influence of seismic loading and construction stage effects on reinforced concrete buildings incorporating transfer beams and floating columns. These findings clearly indicate that conventional analysis methods may significantly underestimate structural demand, potentially leading to unsafe design if construction stage effects are ignored. Therefore, a clear research gap exists regarding the seismic behavior of reinforced concrete solid slab structures incorporating transfer beam systems when construction stage effects are considered. In addition, the influence of transfer beam geometry, continuity, and in-plan location on both local structural response and global seismic performance remains insufficiently explored in the available literature.

In summary, previous studies have primarily focused on the gravity load behavior of transfer systems or simplified seismic analyses, with limited consideration of the combined effects of construction sequencing, slab–beam interaction, and floating column systems. Moreover, most existing research assumes fully constructed structures subjected to instantaneous loading, which does not accurately represent real construction processes. These limitations highlight the need for integrated analytical approaches that consider both seismic loading and staged construction effects. To address these limitations, the present study conducts a comprehensive numerical investigation of the seismic behavior of reinforced concrete multi-story buildings incorporating transfer beam systems and floating columns within solid slab floor systems using Equivalent Static Analysis (ESA), Response Spectrum Analysis (RSA), and Construction Stage Analysis (CSA) in ETABS.

The novelty of the present study lies in its integrated analytical framework that simultaneously addresses three aspects not previously examined in combination: (i) the seismic behavior of reinforced concrete solid slab structures incorporating transfer beam systems and floating columns, (ii) the explicit incorporation of Construction Stage Analysis (CSA) alongside conventional seismic methods (ESA and RSA) to capture time-dependent load redistribution effects, and (iii) a systematic parametric investigation of transfer beam size, continuity, and in-plan location within a unified comparative framework. Unlike most existing studies that adopt simplified static analyses or focus exclusively on gravity loading, the present work provides quantitative design-oriented insights applicable to practical seismic design of buildings with transfer floor systems.

1.1 Research Gap

Despite the extensive research conducted on transfer systems in reinforced concrete buildings, several important aspects remain insufficiently explored. Most previous studies have primarily focused on the gravity load behavior of transfer beams or on simplified seismic analyses that do not fully capture the complex interaction between structural components within transfer floor systems. In particular, limited attention has been given to reinforced concrete buildings incorporating floating columns supported by transfer beams within solid slab floor systems, despite the increasing adoption of such configurations in modern multi-story construction [1,4].

Furthermore, many existing investigations evaluate structural response assuming that the structure is fully completed and subjected to simultaneous loading. However, in real construction scenarios, structural elements are erected sequentially, and loads are progressively applied during construction. This staged development of the structure may significantly influence the redistribution of internal forces, particularly in systems containing transfer beams where large, concentrated loads are transmitted through discontinuous load paths [14–16]. Although, Construction Stage Analysis (CSA) has been recognized as an effective approach for capturing the influence of construction sequencing and time-dependent effects such as creep and shrinkage, its integration with seismic assessment of reinforced concrete buildings containing transfer beams and floating columns has been only marginally investigated in previous studies [19].Additionally, the interaction between transfer beams and solid slab systems under seismic loading conditions has not been systematically examined in the available literature. While several studies have investigated transfer girders or transfer slabs, the role of slab–beam interaction in controlling force redistribution, deformation patterns, and overall seismic performance of buildings with floating columns remains insufficiently understood.

Therefore, a clear research gap exists in understanding the combined influence of transfer beam geometry, structural continuity, in-plan location, and construction stage effects on the seismic behavior of reinforced concrete buildings incorporating floating columns within solid slab systems. Addressing this gap is essential for improving the reliability of structural analysis and developing more effective design strategies for buildings containing transfer floor systems in seismic regions. Accordingly, the present study is positioned to address this unresolved gap through an integrated seismic and staged-construction assessment framework for transfer beam systems in reinforced concrete solid slab buildings with floating columns.

1.2 Objectives of Study

In order to address the identified research gaps, this study aims to conduct a comprehensive numerical investigation of the seismic behavior of reinforced concrete multi-story buildings incorporating transfer beam systems and floating columns within solid slab floor structures. The specific objectives of this study can be summarized as follows:

- Seismic performance evaluation of transfer beam systems: To evaluate the seismic response of reinforced concrete buildings incorporating floating columns supported by transfer beams and to compare their behavior with conventional structures without vertical irregularities.
- Assessment of construction stage effects on seismic response: To investigate the influence of construction sequence and staged loading on structural response by integrating Construction Stage Analysis (CSA) with conventional seismic analysis methods, including Equivalent Static Analysis (ESA) and Response Spectrum Analysis (RSA).
- Parametric investigation of transfer beam characteristics: To systematically examine the influence of key design parameters of transfer beams, including beam dimensions, structural continuity, and in-plan location, on internal force distribution, structural deformation, and overall seismic behavior.
- Evaluation of load redistribution mechanisms: To analyze the redistribution of axial forces in columns and the interaction between transfer beams, floating columns, and surrounding structural elements in order to better understand seismic load transfer mechanisms within buildings containing transfer floor systems.
- Development of practical design insights: To provide structural design insights and practical recommendations, based on analytical findings, for the safe and efficient implementation of transfer beam systems in reinforced concrete buildings subjected to seismic loading.

2. Methodology

2.1. Methods of analysis

The effect of design earthquake loads on structures can be assessed using three main analytical methodologies: Equivalent Static Analysis (ESA), Response Spectrum Analysis (RSA), and Construction Stage Analysis (CSA).The selection of these three methods is based on their ability to capture complementary aspects of structural behavior, namely simplified global response (ESA), dynamic modal response (RSA), and time-dependent construction effects (CSA), thereby providing a comprehensive assessment of seismic performance. This combined analytical strategy also enables direct comparison between conventional elastic seismic assessment and staged-construction-based response, which is essential for quantifying demand amplification in transfer beam systems.

In ESA, seismic forces are represented by an equivalent lateral load assumed to reflect the dynamic action of earthquake excitation. The base shear, representing the total horizontal force acting on the structure, is determined as a function of the building mass, fundamental period of vibration, and structural characteristics. According to code provisions, this shear is distributed along the building height in proportion to the lateral force distribution pattern. This method is generally considered conservative for low- to mid-rise buildings with regular configurations [19].

The RSA represents the peak response of a set of single-degree-of-freedom oscillators subjected to the same base excitation, each characterized by a different natural frequency. This approach enables the evaluation of structural response within the linear elastic range by considering modal contributions. As stated in ECP (201-2012) [20], the analysis must capture at least 90% of the total mass participation to ensure that all significant vibration modes are included, thereby improving the accuracy of the predicted seismic response [20,21].

CSA facilitates the simulation of the staged construction process by incorporating structural elements and loads sequentially [22]. The progressive application of loads during construction can result in significantly different internal force distributions compared to conventional analysis approaches where loads are applied after full structural completion, as shown in Fig. 1.

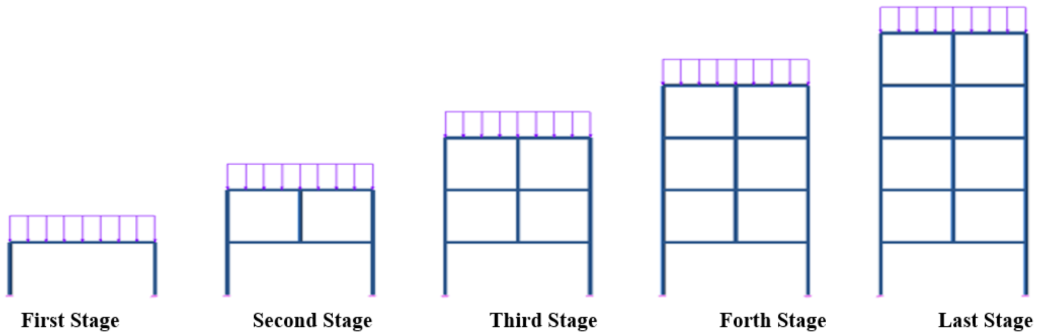

Fig. 1 Stage formation in construction sequence analysis (CSA)

All analyses (ESA and RSA) were performed assuming linear elastic structural behavior with cracked section stiffness modifiers in accordance with ECP 203 provisions, while CSA additionally incorporates time-dependent effects. No material or geometric nonlinear analysis was considered, as the objective of this study is to perform a comparative evaluation of structural response within the elastic range.

The CSA approach adopted in this study simulates the sequential activation of structural elements on a story-by-story basis, allowing the accumulation of loads and stiffness development to be realistically captured, which is particularly critical for structures incorporating transfer beams and floating columns. The construction process was modeled using a story-by-story activation scheme, where each stage represents the addition of one floor along with its associated dead loads. This sequential approach enables realistic simulation of load accumulation and stiffness development throughout the construction process.

2.2. Capacity-to-Demand Ratio Evaluation

To provide a more rational assessment of structural performance, the capacity-to-demand ratio (C/D ratio) was introduced as an additional evaluation parameter for transfer beams. While percentage increases are useful for highlighting relative variations between different cases, they do not directly reflect the adequacy or safety margin of structural members. Therefore, the C/D ratio was used to relate the available structural capacity to the corresponding elastic demand obtained from the analysis. The capacity-to-demand ratio was evaluated for both flexure and shear as follows:

- $C/D_{flexure} = \frac{M_{capacity}}{M_{demand}}, C/D_{shear} = \frac{V_{capacity}}{V_{demand}}$

where the demand values were obtained from the elastic analysis results, and the capacities were determined based on the relevant design code provisions.

A C/D ratio greater than unity indicates sufficient capacity, while values approaching or below unity indicate critical or unsafe conditions.

2.3. Description of Modeling and Building

Five models (A*, F, H, K, L) with identical plan areas of 450 m^2 (25 m × 18 m) were analyzed, as detailed in Table 1. Buildings A*–K consist of G+11 stories, while Model L includes a basement (Basement + G + 11). Models A*, F, H, and K include 1.5 m plan extensions on both sides, as shown in Fig. 2. The typical floor height is 3 m, the ground floor is 4 m, and the basement is 3 m.

The adopted building configuration (G+11 stories, regular plan geometry, and dual system with shear walls) represents a typical mid-rise reinforced concrete structure commonly investigated in previous studies addressing vertical irregularities and transfer systems, thereby ensuring consistency with existing literature and practical relevance. Such building configurations have been widely adopted in previous studies investigating vertical irregularities and transfer beam systems under seismic loading conditions [11,12], thereby supporting the selection of the present models. In addition, this structural scale and layout are sufficiently representative to capture the interaction between transfer-level irregularity and global seismic response without introducing excessive geometric complexity. All buildings were designed in accordance with the Egyptian Code ECP 203-2020 [23], with concrete compressive strength fcu = 30 MPa, concrete density of 25 kN/m^3, and steel yield stress of 350 MPa (280 MPa for stirrups). The structural system consists of 120 mm solid slabs supported by beams (250 mm × 500 mm), columns, and six shear walls of 5 m length, corresponding to a shear wall area ratio of 2.29%, as illustrated in Fig. 2 (a, b, c, d). Design loads include a wall load of 6.5 kN/m^2, flooring load of 2 kN/m^2, and live load of 3 kN/m^2.

Table 1. Details of the models

Groups	Model	Subsection numbering	Location of the Transfer Beam	Type of Beam	Section of Beam (mm)	Number of floors
Control	A	A*	—	—	—	Ground + 11 Typical
Group 1	F	F-1	External (At axis A)	Simple	400*500	Ground + 11 Typical
		F-2	External (At axis A)	Simple	800*1000	Ground + 11 Typical
		F-3	External (At axis A)	Simple	800*1400	Ground + 11 Typical
		F-4	External (At axis A)	Simple	800*1600	Ground + 11 Typical
	L	L	External (At axis A)	Simple	800*1600	Basement + Ground + 11 Typical
Group 2	F	F-5	External (At axis A)	Continuous	400*500	Ground + 11 Typical
		F-6	External (At axis A)	Continuous	800*1000	Ground + 11 Typical
		F-7	External (At axis A)	Continuous	800*1400	Ground + 11 Typical
		F-8	External (At axis A)	Continuous	800*1600	Ground + 11 Typical
Group 3	H	H	Internal (At axis B)	Simple	800*1600	Ground + 11 Typical
	K	K	Internal (At axis C)	Simple	800*1600	Ground + 11 Typical

Note: A = control model (without floating column)*

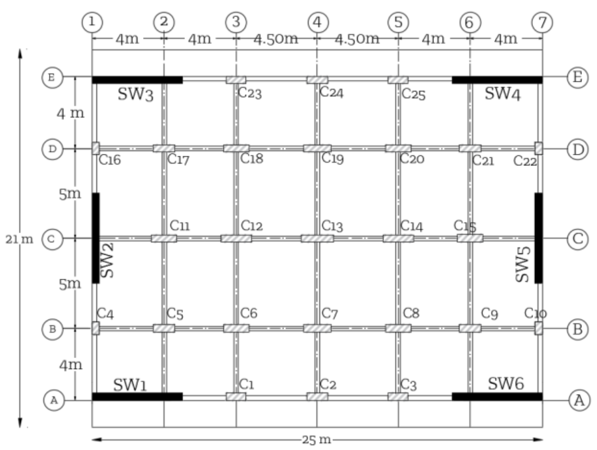

(a) Ground floor plan for model A,F,H and K

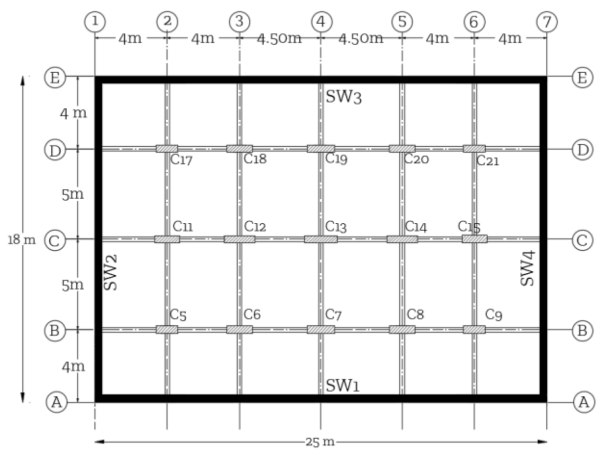

(b) Basement floor plan for model L

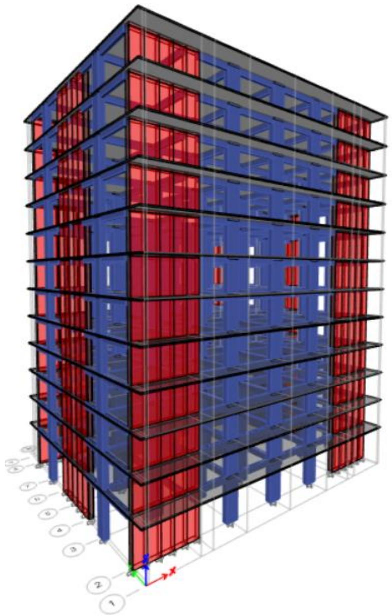

(c) 3D for models A,F,H and K

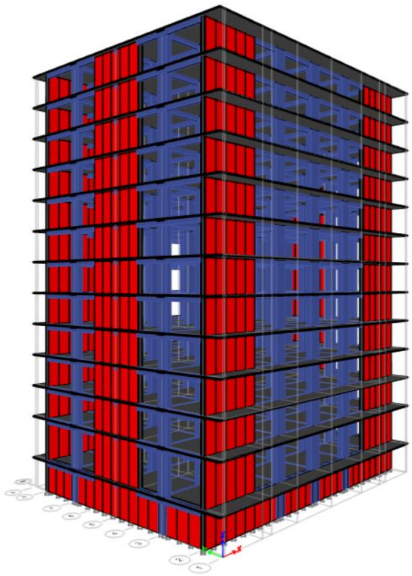

(d) 3D for model L

Fig. 2. Floor plan of proposed building and 3d view of proposed building

2.3.1 Modeling Assumptions and Structural Idealization

- Boundary Conditions: All column bases were modeled as fixed supports, restraining both translational and rotational degrees of freedom.
- Diaphragm Assumption: All floor slabs were assumed to act as rigid diaphragms in-plane, ensuring proper distribution of lateral forces among vertical load-resisting elements.
- Slab Modeling: Slabs were modeled using linear elastic shell elements (membrane + bending behavior) to accurately represent both in-plane stiffness and flexural response.
- Connection Rigidity: Beam-column and slab-beam connections were assumed to be fully rigid, consistent with monolithic reinforced concrete construction practice.

Transfer beams were not modeled as isolated structural members, but rather as integral components of the three-dimensional global structural system developed in ETABS Ultimate 22.0. This modeling approach ensures full interaction between transfer beams, solid slabs, columns, and shear walls, enabling realistic representation of stiffness distribution and load transfer mechanisms throughout the structure. The elastic demand on transfer beams was quantified by extracting critical internal force responses from the global model, including maximum bending moments, maximum shear forces, and vertical deflections, under the governing load combinations for each analysis method. Although CSA incorporates staged loading effects, the structural response at each construction stage is still evaluated based on linear elastic stiffness formulations, thereby providing enhanced but still elastic force demand evaluation, ensuring consistency within the overall analytic.

2.3.2 Material Modeling

All structural elements were modeled assuming linear elastic behavior with cracked section stiffness modifiers in accordance with ECP 203 recommendations to account for stiffness degradation under service-level loading. Time-dependent effects (creep and shrinkage) were not considered in ESA and RSA analyses but were incorporated in CSA using ETABS built-in models, which simulate age-dependent stiffness variation and stress redistribution. This modeling strategy is considered appropriate for comparative seismic assessment within the elastic range, while acknowledging that local nonlinear damage mechanisms are outside the scope of the present investigation.

4.3.3 Parametric Study and Model Classification

The models are grouped into three categories: Group 1 examines transfer beam cross-section effects and basement influence (F-1, F-2, F-3, F-4, L), Group 2 studies beam continuity impact (F-5, F-6, F-7, F-8), and Group 3 evaluates transfer beam location effects (H, K), as shown in Fig. 3. The selected transfer beam cross-sections were chosen to represent a wide range of stiffness conditions, enabling the investigation of structural sensitivity to transfer beam rigidity. Similar parametric variations in transfer beam stiffness have been reported in previous research to significantly influence force redistribution and deformation behavior in structures with discontinuous vertical load paths [4,13]. Specific columns were removed at ground level (Column 2 for Models F and L, Column 7 for Model F, and Column 13 for Model H) with transfer beams added in four different cross-sections as specified in Table 1. The selection of floating column locations reflects commonly observed architectural configurations in practice and is consistent with previously studied cases of vertical irregularity. Previous studies have shown that such configurations lead to increased structural flexibility and concentration of seismic demand at transfer levels [11,12], further justifying their inclusion in this study. All results were compared against the control model A* (without floating column) using ETABS Ultimate 22.0.0 under vertical and lateral loading.

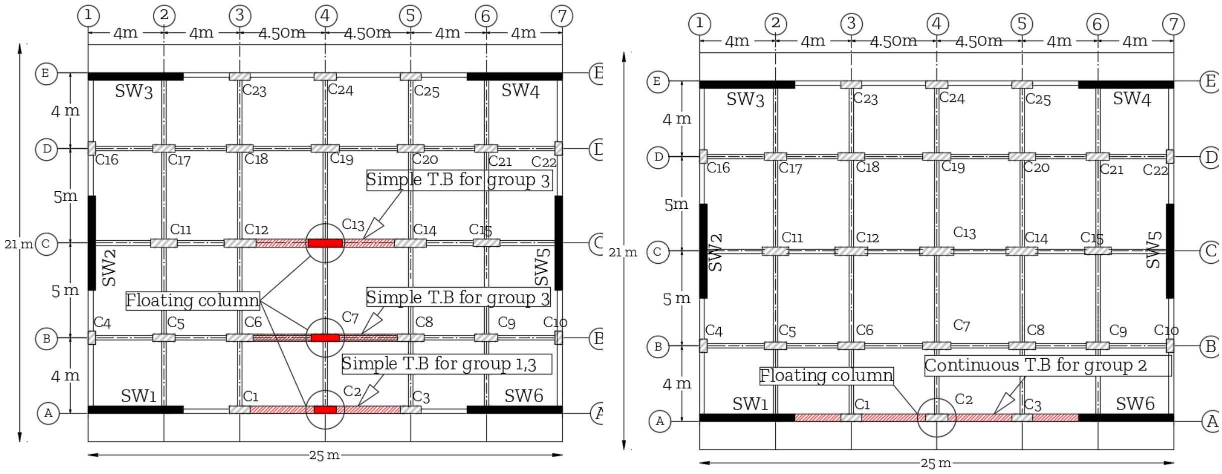

(a) Location of transfer beam relative to slab for groups

(b) Continuity of transfer beam relative to slab for groups

Fig. 3. Location and continuity of transfer beams relative to slab

2.4. Seismic Analysis Framework and Load Combination Methodology

2.4.1 Analysis Framework

This study establishes a seismic analysis framework for buildings in Cairo Governorate (Zone III per ECP 203-2020) [23]. The analysis considers soil type C with the SMRF system and an importance factor of 1.0, as shown in Table 2. These parameters were selected to represent typical seismic design conditions for reinforced concrete buildings in Egypt and to ensure consistency with regional seismic studies. Three seismic analysis methods are employed: ESA, RSA, and CSA. The framework incorporates validation procedures to ensure structural adequacy. Modal analysis confirms cumulative mass participation ratios exceed 90% for all models, and a base shear comparison between ESA and RSA shows VRSA/VESA = 0.89 and 0.86 correlation, validating the approach. All models use identical seismic parameters, as shown in Table 3 for consistent evaluation. This comparison serves as a basic verification of the seismic demand estimation; however, detailed model validation is presented separately in a dedicated section.

Table 2. Code seismic parameters for all models

Seismic parameters		ECP (203-2020) [23]
Soil type		C
Seismic zone & intensity		Third, ag = 0.15 g
Seismic & soil factors		S = 1.50
Occupancy category		II
Importance factor		γ=1.00
Response modification factor		R = 5.0
Live load contribution in W (ΨEi)		25% of LL
Seismic weight W (kN)		64850
Cracked stiffness ratio	Column	0.70
	Shear wall	0.35
	Beam	0.50
	Slab	0.250

Table 3. Code seismic parameters for methods

Seismic parameters	ESA	RSA
Horizontal design response spectrum for elastic structural analysis	Curve for Models TC = 0.25 s, TB = 0.1 s, TD = 1.20 s *Maximum is constant in ECP (203-2020) [18] in only case that T has mass participation ratio greater than 90%.	
General equation Maximum and minimum curve	$2.50 a_g \, S \, \gamma_1$ $0.20 a_g \, \gamma_1$	
Fundamental time period T (s) Ct = 0.05	T^S=$C_t H^{3/4}$ = 0.75	C_t^R = Ct T^R=$C_t^R H^{3/4}$ C_U = 1.2 T_U^R=$C_U T^S$ = 0.9 $T^M (first\ mode)$ = 3.257 T^R=Min $\{\{T_U^R, T^M\}$ = 0.9
Design spectrum acceleration Sd (m/s2)	0.368	0.307
Number of mode shapes	12	
Mass participation ratio (minimum 90%)	X-direction = 0.9852 Y-direction = 0.9883	
Average RSA/ESA shear ratio VRSA/VESA of both directions (Minimum =0.85)	0.89	0.86

2.4.2 Load Combinations

Load combinations follow Egyptian Code specifications, emphasizing Construction Sequence Analysis for construction and service loading stages. In the equivalent static analysis (ESA), eccentricity was included according to the static load combination requirements of ECP-201 as per Clause 8.7.2. of the Egyptian Code (ECP-201) [20], while for the response spectrum analysis (RSA), the combination 100%X + 30%Y + 30%Z was applied following the code's dynamic load provisions as per Clause 8.7.3.5.2 of the Egyptian Code (ECP-201) [20]. Additionally, conventional dead loads were replaced with staged construction loads applied incrementally across phases, as presented in Table 4. This approach ensures that both static and dynamic load effects are accurately represented and provides a realistic assessment of structural response throughout construction and service life. This approach allows realistic simulation of load accumulation and internal force redistribution during construction, which is particularly important for transfer beam systems subjected to early-age loading effects.

Table 4. Combinations of loads for methods

Methods	Load combinations	
Vertical loads	1.4 D.L + 1.6 L.L	2. 1.4 D.L
ESA	1. 1.12 Total D.L + αL.L ± EQx	7. 0.9 Total D.L ± EQx
	2. 1.12 Total D.L + αL.L ± EQy	8. 0.9 Total D.L ± EQy
	3. 1.12 Total D.L + αL.L ± (EQx + ecc)	9. 0.9 Total D.L ± (EQx + ecc)
	4. 1.12 Total D.L + αL.L ± (EQx − ecc)	10. 0.9 Total D.L ± (EQx − ecc)
	5. 1.12 Total D.L + αL.L ± (EQy + ecc)	11. 0.9 Total D.L ± (EQy + ecc)
	6. 1.12 Total D.L + αL.L ± (EQy − ecc)	12. 0.9 Total D.L ± (EQy − ecc)
RSA	1. 1.12 Total D.L + αL.L + R.SX + 0.3 R.SY + 0.3 R.SZ	4. 0.9 Total D.L + R.SX + 0.3 R.SY + 0.3 R.SZ
	2. 1.12 Total D.L + αL.L + R.SY + 0.3 R.SX + 0.3 R.SZ	5. 0.9 Total D.L + R.SY + 0.3 R.SX + 0.3 R.SZ
	3. 1.12 Total D.L + αL.L + 0.3 R.SY + 0.3 R.SX + R.SZ	6. 0.9 Total D.L + 0.3 R.SY + 0.3 R.SX + R.SZ
CSA	1. 1.12 CSA + αL.L ± EQx	10. 0.9 CSA ± EQx
	2. 1.12 CSA + αL.L ± EQy	11. 0.9 CSA ± EQy
	3. 1.12 CSA + αL.L ± (EQx + ecc)	12. 0.9 CSA ± (EQx + ecc)
	4. 1.12 CSA + αL.L ± (EQx − ecc)	13. 0.9 CSA ± (EQx − ecc)
	5. 1.12 CSA + αL.L ± (EQy + ecc)	14. 0.9 CSA ± (EQy + ecc)
	6. 1.12 CSA + αL.L ± (EQy − ecc)	15. 0.9 CSA ± (EQy − ecc)
	7. 1.12 CSA + αL.L + R.SX + 0.3 R.SY + 0.3 R.SZ	16. 0.9 CSA + R.SX + 0.3 R.SY + 0.3 R.SZ
	8. 1.12 CSA + αL.L + R.SY + 0.3 R.SX + 0.3 R.SZ	17. 0.9 CSA + R.SY + 0.3 R.SX + 0.3 R.SZ
	9. 1.12 CSA + αL.L + 0.3 R.SY + 0.3 R.SX + R.SZ	18. 0.9 CSA + 0.3 R.SY + 0.3 R.SX + R.SZ

2.5. Numerical Stability, Convergence, and Sensitivity Considerations

A consistent finite element discretization strategy was adopted across all models to ensure unbiased comparison. Slabs were modeled using shell elements, while beams and columns were modeled using frame elements. Although a formal mesh convergence study was not conducted, the selected mesh density follows established ETABS modeling guidelines and is considered sufficient for capturing global structural response. The absence of a detailed sensitivity analysis is acknowledged as a limitation; however, the use of identical modeling assumptions across all cases ensures that comparative results remain valid and reliable.

2.6. Response Parameters and Performance Evaluation

Structural performance was evaluated using both global and local response parameters.

- Global response: base shear, inter-story drift, lateral displacement
- Local response: transfer beam bending moments, shear forces, deflections, and column axial forces

In addition to absolute response values, capacity-to-demand (C/D) ratios were evaluated based on code-defined limits to assess structural adequacy and safety under seismic loading. This allows the results to be interpreted not only in a comparative manner but also in terms of structural performance and compliance with design requirements.

3. Verification of Numerical Models

The validity of the adopted numerical modeling methodology was verified through comparison with a well-established benchmark study of a reinforced concrete building incorporating transfer girders, as reported by Osama O. El-Mahdya et al. [24]. The theoretical framework was implemented using ETABS to evaluate its capability to accurately capture both global and local seismic response characteristics of structural systems equipped with transfer elements.

3.1. Building Description

The case study considers a 15-story reinforced concrete building with a total height of 51.10 m, designed and constructed in Egypt. The structural system consists of reinforced concrete moment-resisting frames, incorporating transfer girders with cross-sectional dimensions of 1500 mm × 2000 mm located at the sixth floor (elevation 21.70 m), corresponding to approximately 43% of the total building height. This configuration introduces a pronounced vertical irregularity near mid-height. Concrete grade C40 was adopted for all structural elements, with yield strengths of 400 MPa for longitudinal reinforcement and 240 MPa for stirrups.

3.2. Seismic Input Data

Seismic analysis was carried out using the response spectrum method in accordance with Eurocode 8 (EN 1998-1), adopting a Type 2 elastic response spectrum. A design ground acceleration of 0.15g and Soil Type C were assumed. The building was classified as Importance Class II with an importance factor $\gamma I = 1.0$, and a response modification factor $R = 5$ was used to represent the expected ductile behavior of the reinforced concrete frame system.

3.3. Analysis Results

The seismic behavior of the building was evaluated through linear response spectrum and nonlinear static analyses, focusing on key response parameters including story displacement, inter-story drift, story shear, and bending moments. Comparative results demonstrate close agreement between the developed numerical model and reference data, confirming the accuracy and reliability of the adopted modeling approach in capturing the seismic response of structures incorporating transfer girders.

3.4. Seismic Response Comparison

3.4.1 Story Shear Distribution

Figures 4 and 5 compare the story shear force distributions in the X- and Y-directions obtained from the reference study and the developed numerical model. In both directions, the shear profiles exhibit a physically consistent trend, with maximum shear demands at the lower stories followed by a progressive reduction toward the upper levels. Quantitative comparisons indicate close agreement across all story levels, with deviations generally within 3%–7%. Slightly higher percentage differences at upper stories are attributed to the reduced magnitude of shear forces. Overall, the results confirm the capability of the numerical model to accurately capture the vertical distribution of seismic shear forces.

3.4.2 Overturning Moment

The overturning moment profiles about the X- and Y-axes, presented in Figures 6 and 7, show strong consistency between the reference and verification results. In both directions, maximum moments occur at the lower stories due to cumulative lateral force effects, followed by a gradual reduction with height. The quantitative comparison demonstrates that the developed model reproduces the reference moment distributions with acceptable deviations, generally ranging between 4% and 7%. These minor differences are attributed to modeling and discretization assumptions rather than to fundamental behavioral discrepancies.

3.4.3 Inter-Story Drift

Figures 8 and 9 illustrate the inter-story drift profiles in both principal directions. The drift response exhibits a nonlinear distribution along the building height, with peak drift demands occurring near mid-height, reflecting stiffness variation and higher-mode effects. The verification results closely match the reference data, accurately capturing both the magnitude and location of maximum drift demands. deviations are generally within 4%–7%, confirming the numerical model's reliability in reproducing global drift behavior.

3.4.4 Story Displacement

The story displacement profiles in the X- and Y-directions, presented in Figures 10 and 11, demonstrate close agreement between the reference and verification models. The displacement response increases progressively with height, exhibiting nonlinear behavior near the base and an approximately linear trend along the upper stories. discrepancies between the two datasets remain within acceptable limits, typically 3% to 7%, and are mainly due to numerical approximations. The results confirm the accuracy of the developed model in capturing the global displacement response under seismic loading. Overall, the verification results demonstrate that the developed numerical model reproduces the reference global response with acceptable agreement, with typical deviations generally remaining within 3%–7% for story shear, overturning moment, drift, and lateral displacement. This level of agreement provides sufficient confidence in the adopted modeling framework for the subsequent parametric assessment of transfer beam systems.

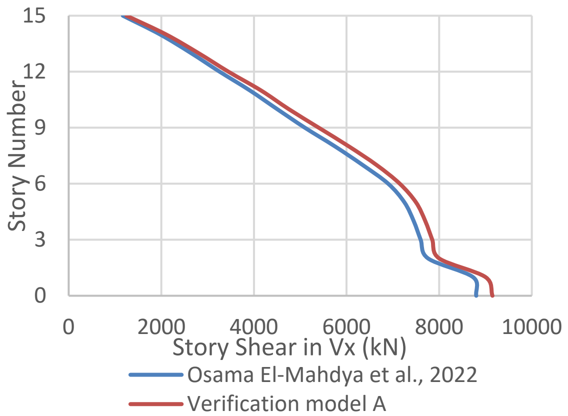

Fig. 4. Comparison of story shear distribution in the X-direction

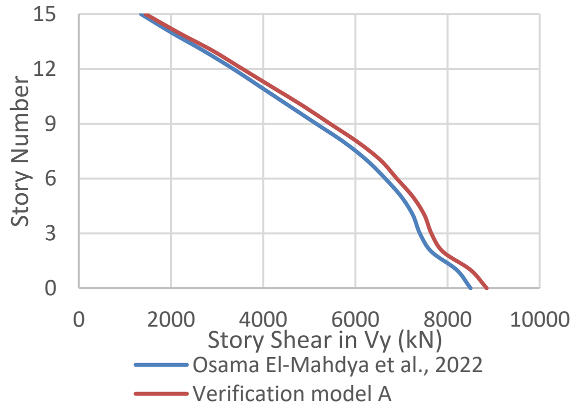

Fig. 5. Comparison of story shear distribution in the Y-direction

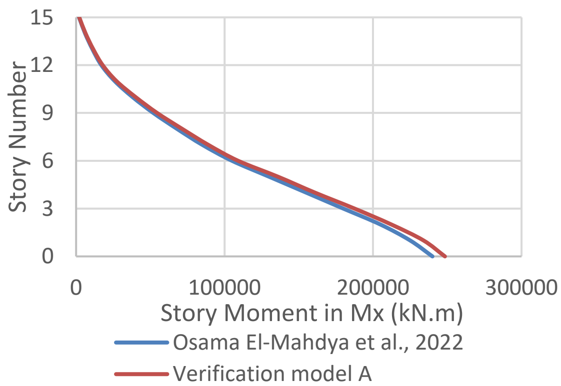

Fig. 6. Comparison between reference and verification overturning moment profiles about the X-axis (MX) along the building height under seismic loading

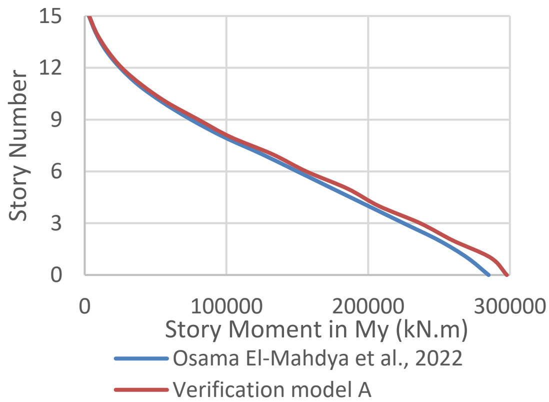

Fig. 7. Comparison between reference and verification overturning moment profiles about the Y-axis (MY) along the building height under seismic loading

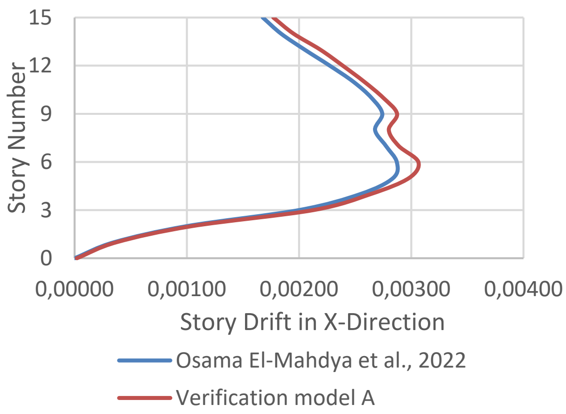

Fig. 8. Comparison of Reference and Verification Story Drift in the X-Direction

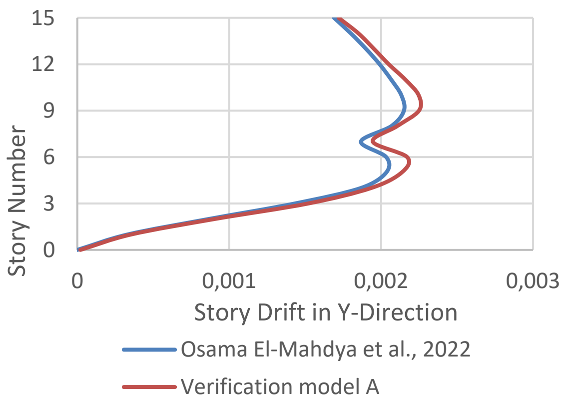

Fig. 9. Comparison of Reference and Verification Story Drift in the Y-Direction

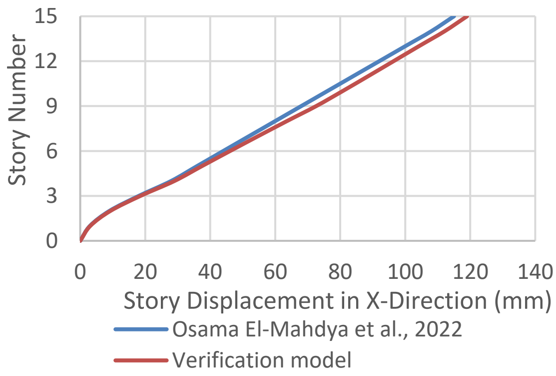

Fig. 10. Comparison of Reference and Verification Story displacement in the X-Direction

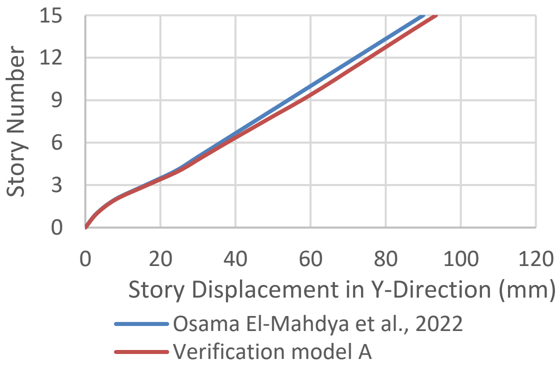

Fig. 11. Comparison of Reference and Verification Story displacement in the Y-Direction

4. Numerical Results and Discussion

The results of this study are systematically presented and analyzed along four primary axes to comprehensively evaluate the structural performance under various design scenarios and analysis methods.

- First axis – transfer beam performance: This axis focuses on the detailed analysis of transfer beams by examining the internal forces they experience, specifically bending moments, shear forces, and vertical deflections. The results are evaluated against allowable code limits to determine the adequacy and serviceability of the beams. All analyses are conducted using three established structural analysis techniques: equivalent static analysis (ESA), response spectrum analysis (RSA), and construction sequence analysis (CSA), allowing for a robust comparison of structural response under realistic loading and construction scenarios.
- Second axis – column load redistribution: The second axis addresses the axial forces developed in columns resting on transfer beams. This is particularly critical in floating columns, where abrupt load transitions occur, affecting the stress distribution in the beams and supporting members.
- Third axis – Effect of transfer beams on the structural behavior of slab beams: This part examines how the presence of transfer beams alters the internal force distribution and deformation characteristics of slab beams, particularly those connected to or located near the transfer level. The analysis focuses on variations in shear forces, bending moments, and vertical deflections of slab beams. In addition, the deformation behavior of solid slabs at the transfer level is evaluated to assess the influence of transfer beams on slab stiffness and load redistribution.

- Fourth axis – structural behavior of the building: This part investigates the overall behavior of the structural system in terms of lateral displacement, inter-story drift, and base shear. These parameters are essential for assessing the structure's seismic performance and lateral stability under different loading scenarios.

4.1. Transfer beam performance: Bending moment, shear force and deflections for transfer beams

The following results represent the elastic internal force demands obtained from the global structural analysis model for transfer beams under the governing load combinations. Group 1 evaluates simply supported reinforced concrete transfer beams integrated with a solid slab system, with beam sections ranging from 40×50 cm (F-1) to 80×160 cm (F-4), while Model L adopts the F-4 section with an additional basement floor. The results show that increasing the transfer beam depth leads to a clear reduction in vertical deflections, accompanied by increases in bending moments and shear forces under both ESA and RSA. Construction Stage Analysis (CSA) consistently produces higher responses than ESA and RSA, confirming the pronounced influence of staged loading, creep, shrinkage, and time-dependent load redistribution, in line with the observations of Durabi & Sunkari, [25] regarding the sensitivity of transfer elements to geometry and construction sequence. In Model F-4, CSA values of bending moment, shear force, and deflection exceed those obtained from RSA by 34.77%, 28.85%, and 5.70%, respectively, while exceeding ESA results by 35.54%, 25.35%, and 57.72%, respectively. Relative to the reference model F-1, CSA results indicate deflection reductions of 66.59%, 78.91%, 82.79%, and 78.69% for models F-2, F-3, F-4, and L, respectively, as shown in Fig. 4. Conversely, bending moments increase by 215.17%, 340.92%, 398.79%, and 389.60%, respectively, as illustrated in Fig. 5, while shear forces rise by 170.35%, 227.67%, 247.80%, and 229.40%, respectively, as presented in Fig. 6. These findings are consistent with previous studies on staged construction effects, which reported that neglecting construction sequencing may lead to significant underestimation of internal forces in transfer elements, particularly due to progressive load accumulation and time-dependent behavior [14,19].

Group 2 examines continuous reinforced concrete transfer beams integrated with a solid slab system (F-5 to F-8). Compared to the corresponding simply supported models in Group 1, the continuous configuration shows improved redistribution of internal actions under Construction Stage Analysis (CSA), particularly for the deeper transfer beams. Under CSA, vertical deflections change by +0.27%, −9.79%, −17.36%, and −16.45% for models F-5 to F-8, respectively (Fig. 7), indicating that continuity becomes more effective in controlling serviceability as the transfer beam stiffness increases. In terms of flexural demand, CSA bending moments change by +0.70%, −4.92%, −11.92%, and −14.10% for F-5 to F-8 (Fig. 8), reflecting the ability of continuous beam–slab systems to redistribute moments and reduce peak flexural demand in stiffer configurations. Conversely, CSA shear forces exhibit slight increases of +0.40%, +2.35%, +2.29%, and +2.65% (Fig. 9), which is consistent with the development of more continuous load paths and higher shear transfer through supports in continuous members.

Overall, these trends confirm that continuity enhances moment redistribution and can improve deflection control—especially in deep transfer beams—while potentially increasing shear transfer demands, which aligns with fundamental structural behavior and common design provisions that associate continuity with reduced flexural peaks and increased support shear demands [7, 23, 26]. This behavior is also in agreement with previous investigations on continuous transfer systems, which demonstrated that continuity enhances moment redistribution and reduces peak flexural demand while increasing shear transfer near supports due to improved load paths [4,13].

Group 3 investigates the effect of transfer beam location within the solid slab system using a constant section (80×160 cm), comparing the peripheral axis (F-4) with an intermediate axis (H) and a more internal axis (K). The results reveal that relocating the transfer beam significantly alters demand distribution rather than producing a monotonic increase toward the core. Under CSA, the intermediate location (H) exhibits the highest deformation and flexural demand, with deflection and bending moment increasing by 55.04% and 45.00%, respectively, relative to F-4 (Figs. 10–11), while the internal axis (K) shows a slightly lower CSA deflection than F-4 (−3.55%) but a higher bending moment (+16.37%). In contrast, shear demand is maximized at the internal axis (K), where

CSA shear force increases by 29.05% compared to F-4, whereas H shows a small reduction in CSA shear (−3.04%) (Fig. 12).

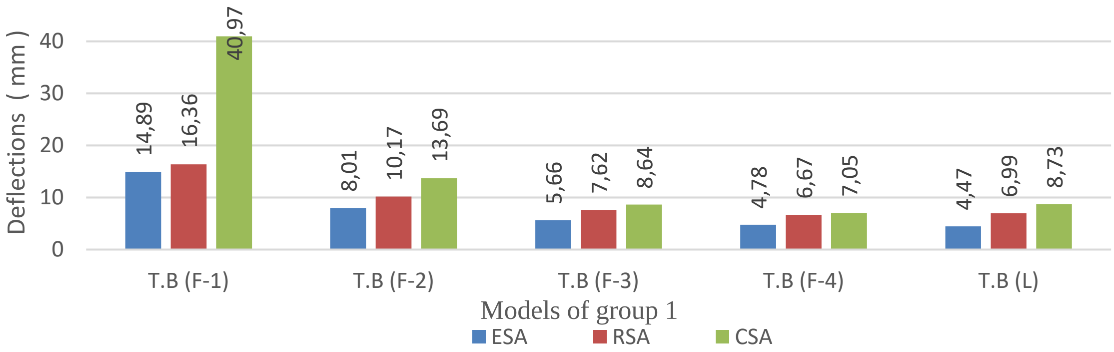

Fig. 4. Comparison of deflection for different analysis for group 1

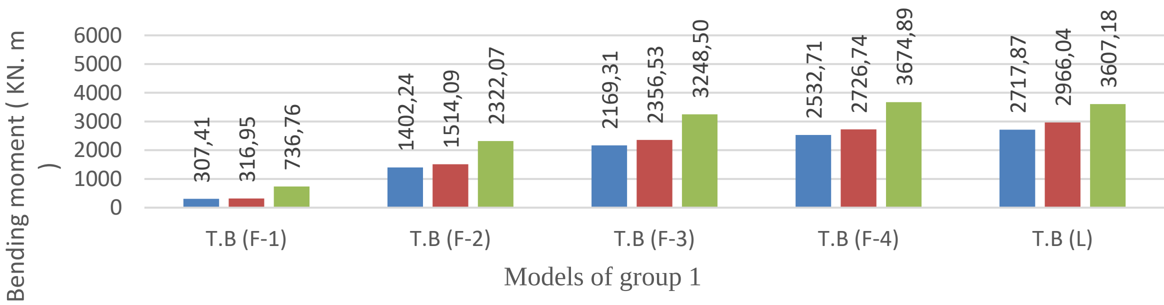

Fig. 5. Bending moment for group 1

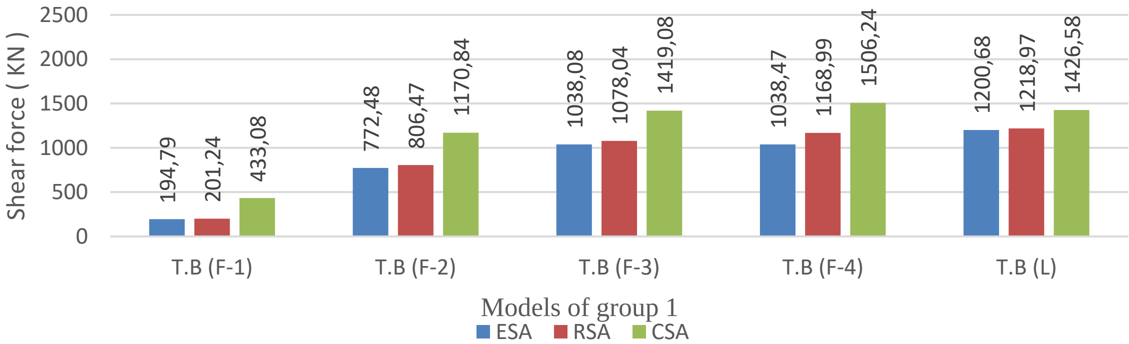

Fig. 6. Shear force for group 1

Across all locations, CSA remains higher than ESA and RSA, confirming the importance of staged loading, creep, shrinkage, and time-dependent redistribution (Figs. 10–12). Structurally, these trends indicate that the H location attracts larger tributary gravity and diaphragm-transferred seismic effects, amplifying flexural response, whereas the K location promotes a more direct force-transfer path and higher support shear concentration, leading to increased shear demand even when deflection is not maximum. Therefore, transfer beam design should explicitly check location-sensitive flexure–shear tradeoffs and construction-stage effects, consistent with the detailing and strength requirements emphasized in ACI 318-19 [7] and ECP 203-2020 [23], and with fundamental seismic demand redistribution concepts described by Chopra, [26]. Similar trends have been reported in previous studies on transfer beam positioning, where the structural response was shown to be highly sensitive to load path configuration and stiffness compatibility, particularly in buildings with vertical irregularities and floating columns [11,13]. Collectively, the results of Groups 1–3 confirm that transfer beam response is governed by the combined effects of stiffness magnitude, continuity condition, and in-plan location. Beam depth primarily controls the balance between serviceability improvement and force amplification, continuity enhances redistribution efficiency, and beam location governs the tributary load path and flexure–shear interaction.

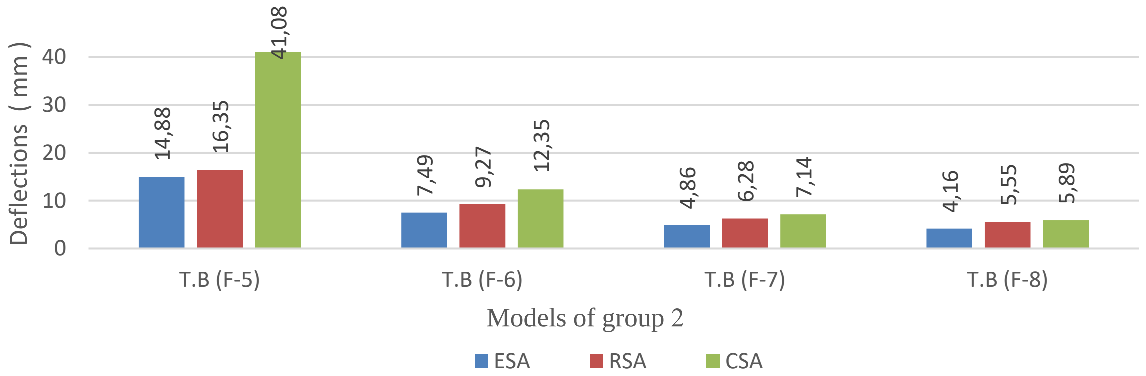

Fig. 7. Comparison of deflection for different analysis for group 2

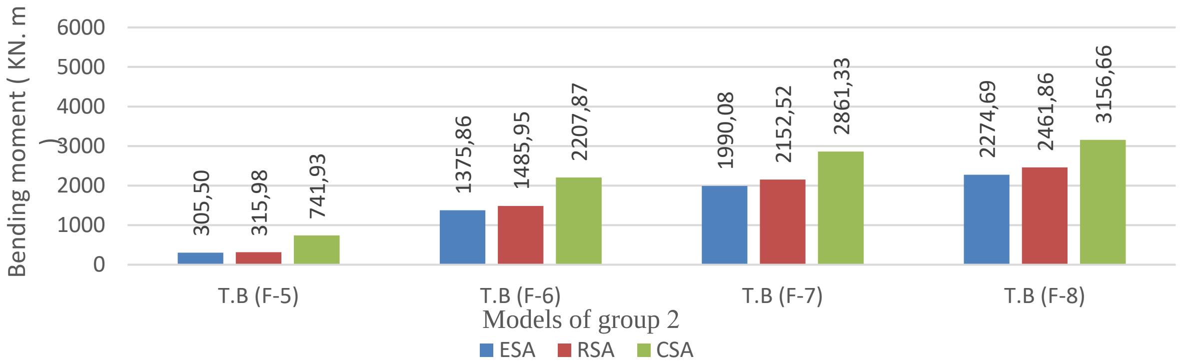

Fig. 8. Bending moment for group 2

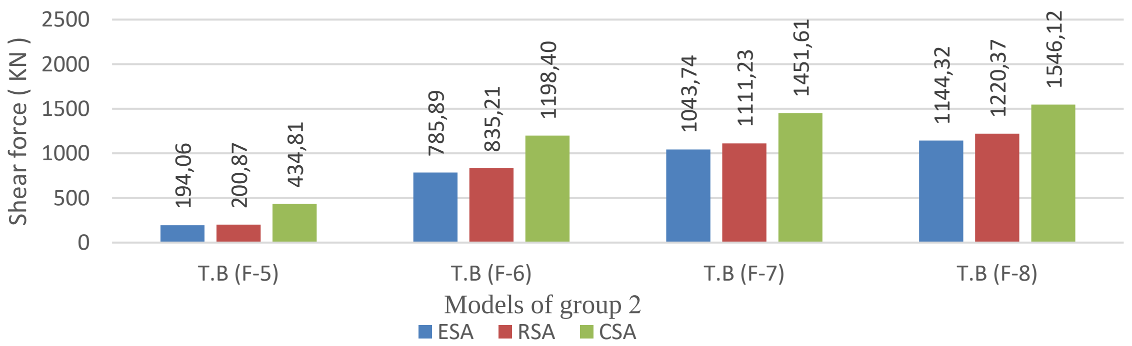

Fig. 9. Shear force for group 2

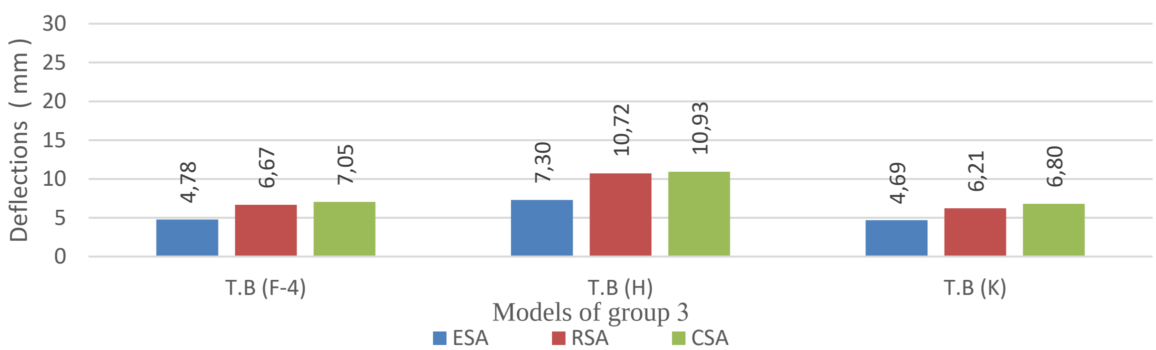

Fig. 10. Comparison of deflection for different analysis for group 3

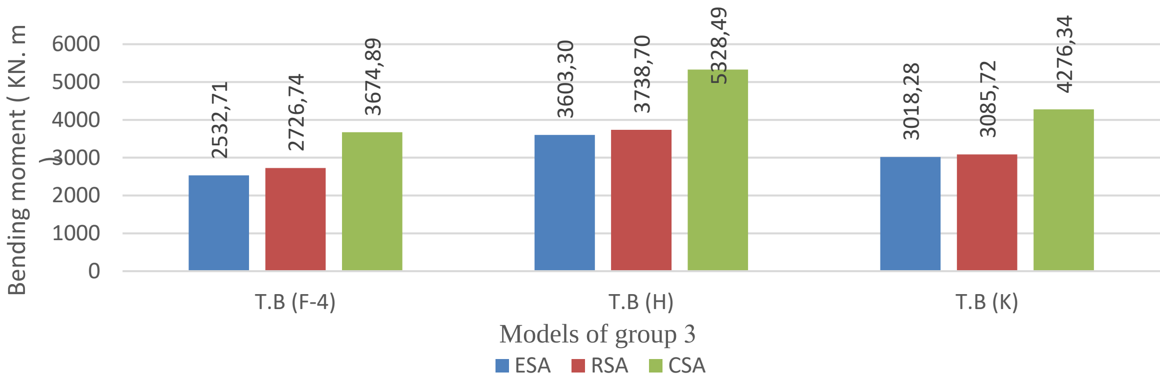

Fig. 11. Bending moment for group 3

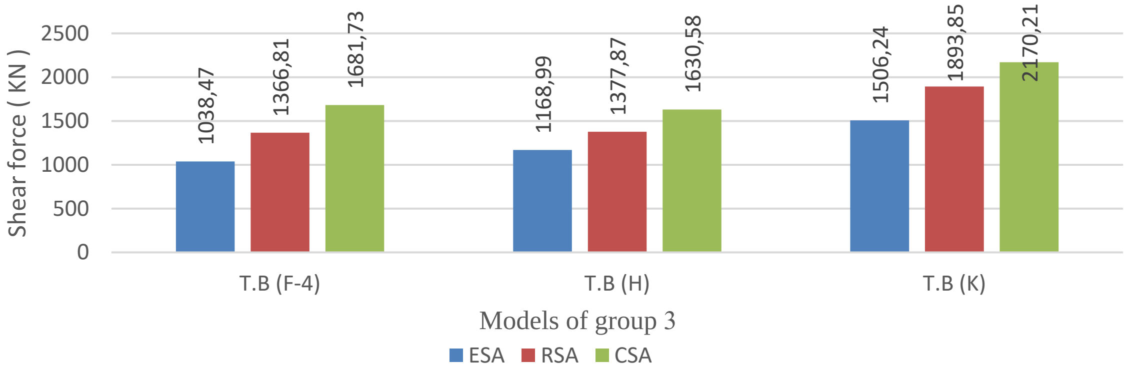

Fig. 12. Shear force for group 3

These observations provide a coherent mechanical explanation for the demand variations observed across the investigated cases. In addition to percentage increase comparisons, the capacity-to-demand ratio (C/D) was evaluated to assess the adequacy of transfer beams under different configurations. The results indicate that although increasing transfer beam depth leads to higher internal force demands due to stiffness-driven load redistribution, the corresponding increase in sectional capacity results in improved C/D ratios, particularly for deeper sections. The shallow transfer beam configurations (e.g., 400×500 mm) exhibit lower C/D ratios, indicating reduced safety margins and potential inadequacy under construction-stage loading. In contrast, deeper sections (e.g., 800×1400 mm and 800×1600 mm) demonstrate significantly higher C/D ratios, confirming their improved structural efficiency and ability to safely resist the increased demands observed under CSA. (Note: C/D ratio trends are consistent with the observed increase in internal forces and beam capacity.)

Table 5 presents the capacity-to-demand ratios for transfer beams under CSA. The results indicate that although internal force demands increase significantly with increasing beam depth, the corresponding increase in sectional capacity results in improved structural performance. The shallow beam configuration (F-1) shows the lowest C/D ratios, indicating a relatively limited safety margin. In contrast, deeper beams (F-3 and F-4) exhibit higher C/D values in both flexure and shear, confirming their superior structural efficiency and ability to safely accommodate increased demands resulting from stiffness-driven load redistribution. These findings demonstrate that evaluating transfer beam performance based solely on percentage increases may be misleading, whereas the C/D ratio provides a more rational and design-oriented assessment of structural adequacy. From a design perspective, these results indicate that section selection should not be judged solely on the basis of force amplification, but rather on the combined basis of demand increase, available capacity, and serviceability compliance under construction-stage conditions. The use of the C/D ratio enables a direct linkage between analysis results and structural design safety, which was not captured by percentage increase comparisons alone.

The deflection assessment of the twelve transfer beam models, considering a span length of 9.0 m, was evaluated against allowable limits specified by local and international design codes, as summarized in Table 6. The results indicate that only models F-1 and F-5 exceed the Egyptian Code allowable deflection limit of L/250 (36.0 mm) under Construction Stage Analysis (CSA), reaching 40.97 mm and 41.08 mm, respectively, as shown in Fig. 13, confirming the inadequacy of these sections for long-span transfer action. Moreover, both models also violate the stricter international serviceability limit of L/500 (18.0 mm) adopted by major standards such as ACI 318-2019, BS 8110-1997, AS 3600-2018, and the typical range implied by Eurocode 2 (EN 1992) [7,27,28,29].

Table 5. Capacity-to-demand ratio for transfer beams (CSA)

Model	Section (mm)	M_demand (kN·m)	M_capacity (kN·m)	C/D (Flexure)	V_demand (kN)	V_capacity (kN)	C/D (Shear)
F-1	400×500	736.76	900	1.22	433.08	600	1.39
F-2	800×1000	2322.07	3000	1.29	1170.84	1600	1.37
F-3	800×1400	3248.50	4200	1.29	1419.08	2000	1.41
F-4	800×1600	3674.89	5000	1.36	1506.24	2300	1.53
L	800×1600	3607.18	5000	1.39	1426.58	2300	1.61

In contrast, the remaining models (F-2, F-3, F-4, L, F-6, F-7, F-8, H, and K) satisfy both the Egyptian and international deflection limits (≤ 18.0 mm), as illustrated in Fig. 13, indicating adequate stiffness within the studied solid slab transfer system. The comparison also highlights that CSA is essential for realistic deflection verification because it captures the amplification associated with creep, shrinkage, and construction sequencing, which may not be fully reflected using ESA or RSA. Based on these findings, adopting a deflection limit of L/500 or less is recommended as a robust serviceability criterion for transfer beam systems in floating-column and high-rise structures to ensure reliable long-term performance.

Table 6. Allowable deflection for a 9.0 m transfer beam based on various codes

Code	Allowable deflection for beam	Allowable deflection for transfer beam	Evaluation of transfer beam deflection against allowable limits (mm)
(ECP 201-2020)	L/250	-	9000 / 250 = 36.0
ACI 318 (USA)	L/360 to L/480	L/500	9000 / 500 = 18.0
BS 8110 (UK)	L/250	L/500	9000 / 500 = 18.0
Eurocode 2	No fixed limit	L/500 - L/1000	9 – 18 typical
AS 3600 (Australia)	L/250	L/500	9000 / 500 = 18.0

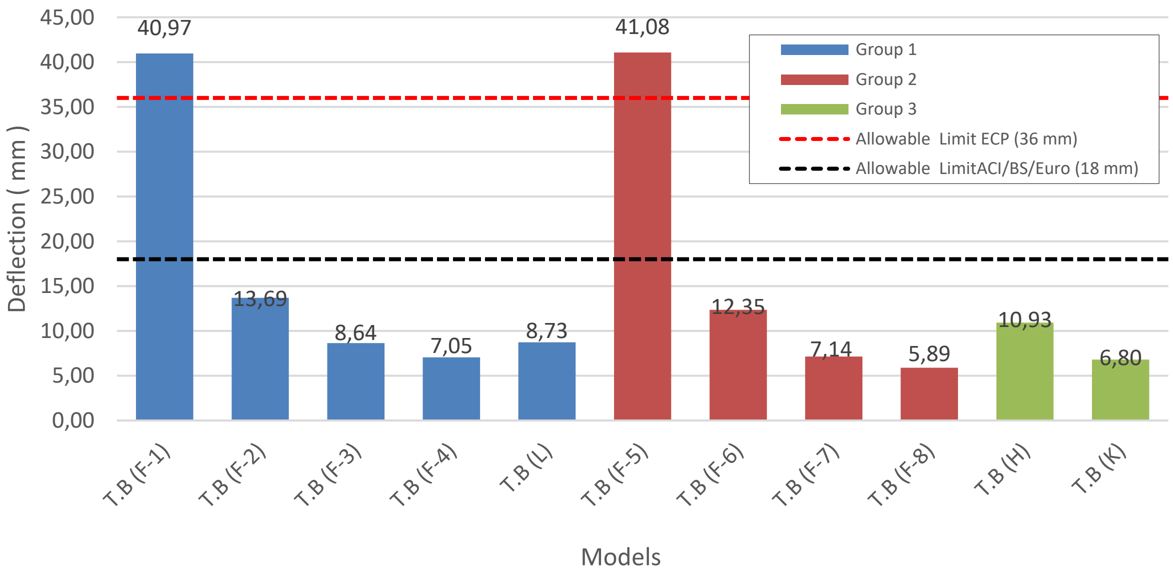

Fig. 13. Beams deflection per Model Vs. allowable limit

4.2. Axial Force for Columns

Table 7 presents the depth of all studied columns, which were intentionally kept uniform across all models to isolate the effect of the transfer mechanism on axial force behavior. All columns have a width of 400 mm, except for columns 1, 3, 6, 8, 12, and 14 in all models, which are 800 mm wide. The following sections discuss significant variations in axial forces caused by the discontinuity beneath floating columns and the resulting load redistribution through adjacent members. Fig. 14 illustrates the locations of the planted columns in the three groups and along different structural axes: Column No. 2 is planted in Groups 1, 2, and 3 along axis A-A, while Columns No. 7 and 13 are planted in Group 3 along axes B-B and C-C.

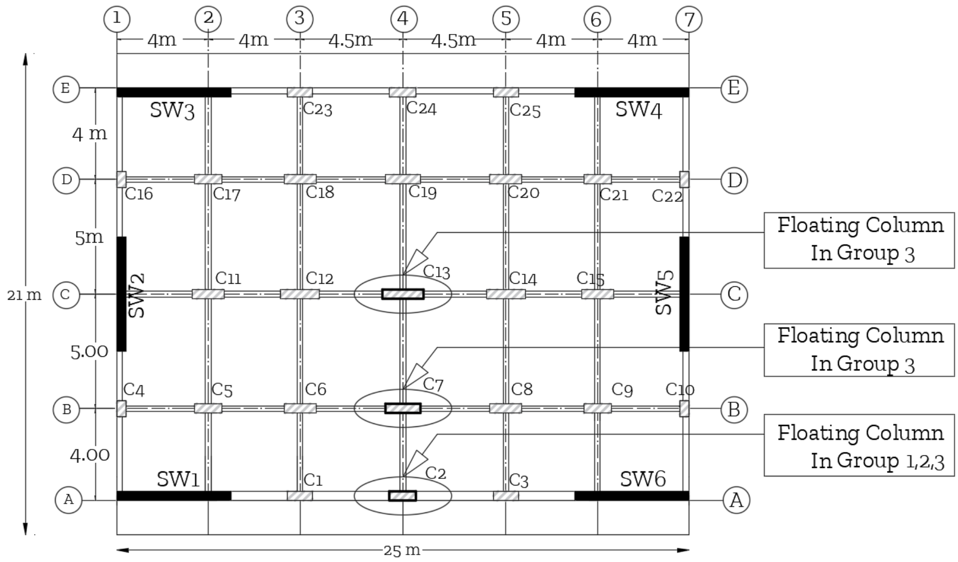

Fig. 14. Locations of the floating column on the axes

Table 7. Column sections for all structural models (Depth)

Col No	Model (mm) A	F-1	F-2	F-3	F-4	L	F-5	F-6	F-7	F-8	H	K
C1	1100	700	700	700	700	800	700	800	800	800	1000	1000
C2	1300	700	700	700	700	700	700	700	700	700	1300	1100
C3	1100	700	700	700	700	800	700	800	800	800	1000	1000
C4	700	800	800	800	800	800	800	800	800	800	800	800
C5	1200	1200	1200	1200	1200	1200	1200	1200	1200	1200	1200	1200
C6	1400	1400	1400	1300	1300	1300	1400	1400	1300	1300	1000	1300
C7	1500	1700	1600	1500	1500	1500	1700	1600	1500	1500	800	1500
C8	1400	1400	1400	1300	1300	1300	1400	1400	1300	1300	1000	1300
C9	1200	1200	1200	1200	1200	1200	1200	1200	1200	1200	1200	1200
C10	700	800	800	800	800	800	800	800	800	800	800	800
C11	1400	1300	1300	1300	1300	1300	1300	1300	1300	1300	1300	1300
C12	1700	1500	1500	1500	1500	1500	1500	1500	1500	1500	1500	1100
C13	1800	1500	1600	1500	1500	1500	1500	1500	1500	1500	1700	900
C14	1700	1500	1500	1500	1500	1500	1500	1500	1500	1500	1500	1100
C15	1400	1300	1300	1300	1300	1300	1300	1300	1300	1300	1300	1300
C16	700	800	800	800	800	800	700	800	800	800	800	800
C17	1200	1200	1200	1200	1200	1100	1200	1200	1200	1200	1200	1200
C18	1400	1300	1300	1300	1300	1300	1300	1300	1300	1300	1300	1300
C19	1500	1400	1400	1400	1400	1400	1400	1400	1400	1400	1400	1500
C20	1400	1300	1300	1300	1300	1300	1300	1300	1300	1300	1300	1300
C21	1200	1200	1200	1200	1200	1100	1200	1200	1200	1200	1200	1200
C22	700	700	800	800	800	800	700	800	800	800	800	800
C23	1100	1000	1000	1000	1000	1000	1000	1000	1000	1000	1000	1000
C24	1300	1100	1100	1100	1100	1100	1100	1100	1100	1100	1100	1100
C25	1100	1000	1000	1000	1000	1000	1000	1000	1000	1000	1000	1000

The axial load distribution for Group 1 illustrates the structural response following the removal of column No. 2 at the ground floor and the introduction of transfer beams with varying stiffness, as shown in Fig. 14. Compared to the reference Model A, column C2 experiences a pronounced reduction in axial load, decreasing from 4870.57 kN to 637.35 kN, 1607.04 kN, 2179.60 kN, 2857.93 kN, and 2420.39 kN in models F-1, F-2, F-3, F-4, and L, respectively. This corresponds to load reductions of approximately 86.9%, 67.0%, 55.3%, 41.3%, and 50.3%, confirming the loss of axial continuity and the redirection of vertical loads through alternative load paths once the column is discontinued.

Conversely, columns directly connected to the transfer beam and aligned with the removed column—particularly columns C1 and C3—exhibit substantial axial load increases. For column C1, axial forces rise from 4308.36 kN in Model A to 6363.05 kN and 6976.41 kN in models F-4 and L, representing increases of approximately 47.7% and 61.9%, respectively. A similar trend is observed in column C3, where axial loads increase from 4308.35 kN to 6363.03 kN and 6976.29 kN, indicating that these columns become the primary vertical load-carrying alternatives as transfer beam stiffness increases. In addition, more distant columns, such as C7 and C13, also show moderate axial load amplification, reflecting the participation of the surrounding frame and slab diaphragm in redistributing the load throughout the structural system.

This redistribution mechanism demonstrates that, in the absence of vertical continuity, the axial load originally carried by the removed column is redistributed through bending action in the transfer beam, membrane action of the slab, and Vierendeel action within the frame, enabling the system to re-establish equilibrium, as illustrated in Fig. 14. The observed trends are consistent with nonlinear progressive collapse studies reported by Izzuddin et al. [30], which showed that columns lose their axial dominance once alternative load paths are activated due to vertical discontinuities. The results also align with the stiffness-based load sharing principle expressed in Eq. (1) [31], where the portion of load attracted by each element is proportional to its relative stiffness. Accordingly, increasing the flexural rigidity EI of the transfer beam enhances its ability to attract a larger share of redistributed load, leading to increased axial forces in adjacent columns and higher shear and axial demands within the transfer beam itself.

$$\frac{K_i}{\sum K} \propto \frac{P_i}{P_{total}} \quad (1)$$

where P_i is the portion of load attracted by element i of the total load P_{total}, K_i is its stiffness, and $\sum K$ represents the total stiffness of all available paths.

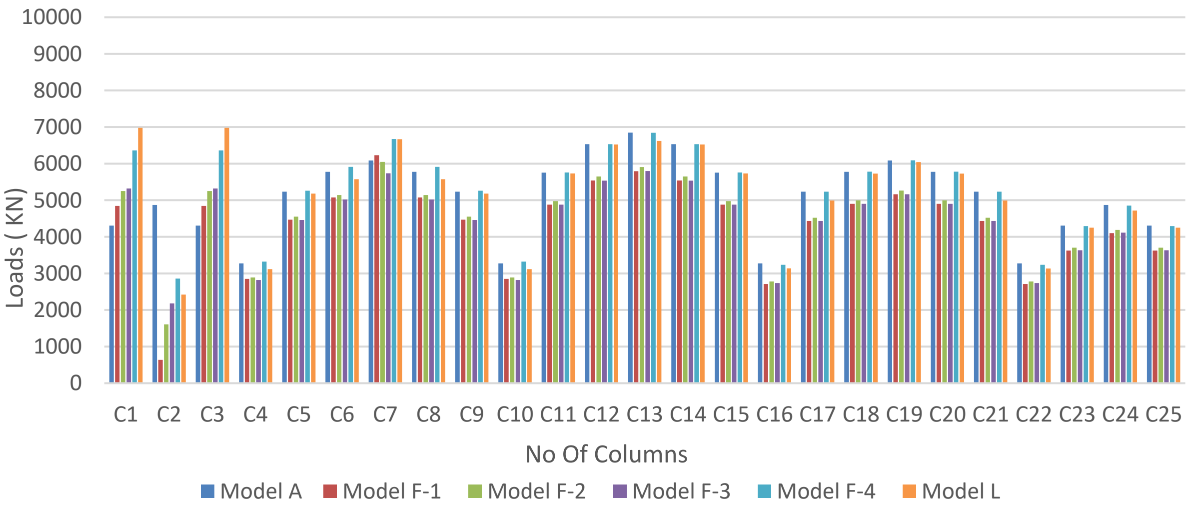

Fig. 15 Axial load for columns of models for groups 1.

In Group 2, the axial load results highlight the influence of transfer beam continuity on vertical load redistribution compared to the reference Model A, as shown in Fig. 16. The floating column C2 exhibits a significant reduction in axial force, decreasing from 4870.57 kN to 644.39 kN, 1739.89

kN, 2436.93 kN, and 2673.94 kN in models F-5, F-6, F-7, and F-8, corresponding to reductions of approximately 86.77%, 64.28%, 49.97%, and 45.11%, respectively. These results indicate that although continuity enhances the transfer beam's ability to attract and redistribute vertical loads, a gradual restoration of axial demand occurs in the floating column as beam stiffness and continuity increase.

Compared to the simply supported models of Group 1, the continuous configurations in Group 2 show a less severe unloading of the floating column, reflecting a more balanced load-sharing mechanism. This behavior is accompanied by axial load increases in adjacent columns directly connected to the transfer beam. For example, column C1 increases from 4308.36 kN to 4903.64 kN, 5503.09 kN, 5852.69 kN, and 5963.56 kN, representing increases of 13.8%, 27.7%, 35.8%, and 38.4% in models B-5 to B-8, respectively, with similar trends observed in column C3. More distant columns, such as C7, exhibit moderate and progressively reduced axial load changes of approximately 2.36%, −3.30%, −6.94%, and −8.22%, indicating that increased continuity limits excessive load transfer to remote frame elements. As illustrated in Fig. 16, these findings confirm that transfer beam continuity governs vertical load redistribution, improving structural integration while leading to a partial recovery of axial forces in the floating column, consistent with stiffness-based load-sharing behavior.

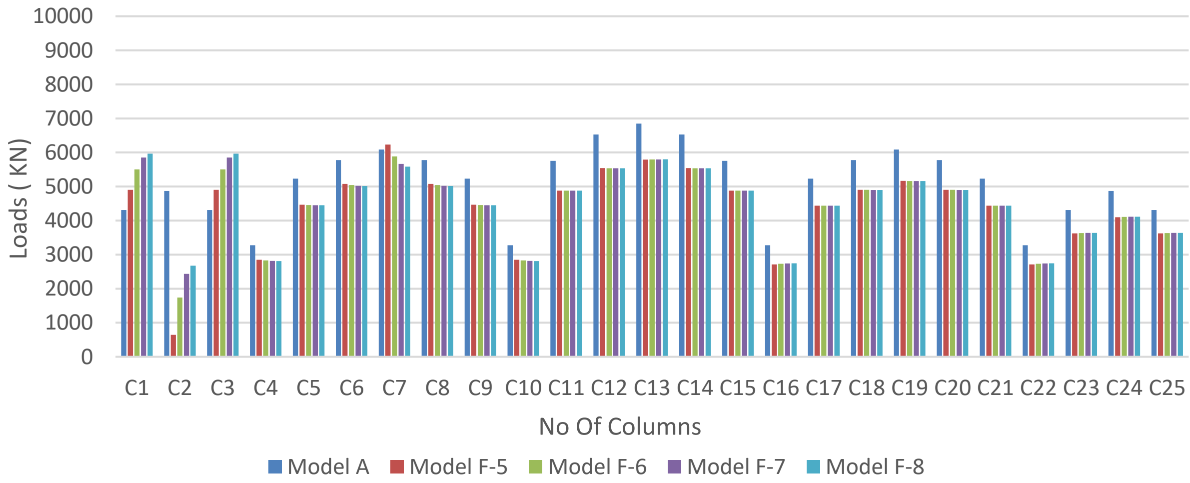

Fig. 16 Axial load for columns of models for group 2

In Group 3, the results demonstrate the influence of transfer beam location on axial force redistribution while maintaining a constant beam cross-section of 80×160 cm in models F-4, H, and K, compared to the reference Model A, as shown in Fig. 17. Relocating the transfer beam from a peripheral position (Model F-4) to intermediate (Model H) and central locations (Model K) results in pronounced changes in axial load distribution across the column grid. The floating column C2 shows a reduction in axial force from 4870.57 kN in Model A to 2857.93 kN in Model F-4, corresponding to a reduction of approximately 41.3%. However, in Model H the axial force increases to 5679.16 kN (i.e., about +16.6% relative to Model A), while Model K nearly restores the original axial demand with 4863.79 kN (a reduction of approximately 0.14%). This indicates that the intermediate beam location does not necessarily provide the most effective unloading of the floating column; instead, the axial response depends on how the beam location reconfigures tributary areas, stiffness compatibility, and alternate load paths within the slab–frame system. At the same time, columns adjacent to and aligned with the transfer beam experience significant axial load redistribution. For example, column C7 changes from 6085.32 kN in Model A to 6674.08 kN in Model F-4 (+9.68%), decreases sharply to 3397.64 kN in Model H (−44.17%), and then rises again to 6515.49 kN in Model K (+7.07%). Central columns such as C12 and C14 exhibit pronounced increases in Model K, reaching 9375.67 kN and 9375.67 kN, respectively, compared to 6530.51 kN in Model A (i.e., increases of about +43.6%), whereas C13 decreases to 3973.66 kN (−42.0%). These trends confirm that modifying the geometric location of the transfer beam alters tributary areas and load paths within the structural system, leading to location-dependent stiffness-driven load sharing and activation of alternate load paths consistent with robustness-oriented design concepts and column-loss redistribution behavior [26, 32, 33].

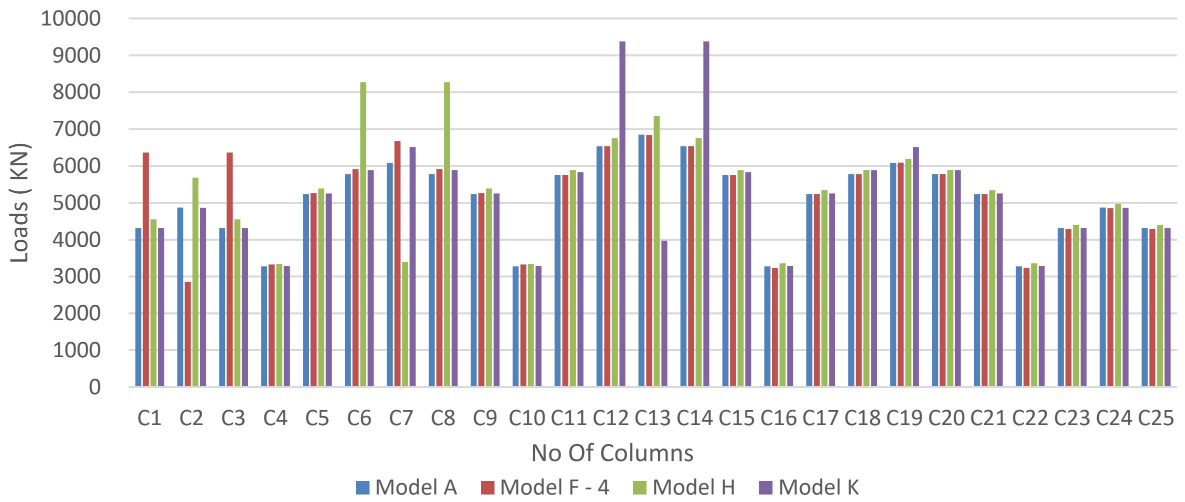

Fig. 17 Axial load for columns of models for group 3

The results highlight that the geometry, continuity, and location of transfer beams play a decisive role in governing axial force redistribution in structures incorporating floating columns. Beams with limited depth or discontinuity exhibit a reduced capacity to redirect vertical loads, thereby increasing the demand on adjacent structural components. In contrast, deeper and stiffer transfer beams attract a larger share of vertical load, enhancing overall stability while imposing higher axial demands on connected members. Structural continuity improves system integration and promotes more balanced load sharing, while moderating excessive unloading of floating columns. Additionally, beam location further influences which structural elements participate most actively in the redistribution process. Collectively, these findings are critical for optimizing transfer beam design to achieve structural safety, efficient load transfer, and robust performance under combined vertical and lateral actions.

6.3. Effect of transfer beams on the structural behavior of slab beams

6.3.1 Structural Response of Slab Beams: Bending Moment, Shear Force, and Deflection

This subsection presents a detailed evaluation of the structural response of slab beams subjected to the presence of transfer beams. The analysis focuses on the variation of bending moments, shear forces, and vertical deflections of slab beams located at different distances from the transfer axis, with particular emphasis on beams directly connected to the transfer beam are summarized in Table 8. The results aim to quantify the degree of force amplification and deformation control induced by the transfer beam system.

As summarized in Table 7, the introduction of transfer beams significantly affects the seismic response of slab beams in solid slab systems, with the magnitude of this effect primarily governed by the transfer beam stiffness and the relative position of the slab beams with respect to the transfer axis. For beam B1 located on Axis A–A and directly aligned with the transfer beam, a pronounced amplification in bending moments is observed. The bending moment amplification factor (AF_M) increases from 1.29 in model F-1 (40 × 50 cm) to a peak value of 2.11 in model F-2 (40 × 100 cm), reflecting the concentration of load transfer and the stiffness discontinuity introduced at the transfer level. With further increases in transfer beam depth in models F-3 and F-4, AF_M decreases moderately to 2.04 and 1.90, respectively, indicating a stiffness saturation effect in which additional flexural rigidity limits further redistribution of bending moments. This behavior is consistent with stiffness-controlled load path mechanisms commonly discussed in seismic design theory [34-36].

Table 8. Maximum bending moment, shear force, and deflection of slab beams under seismic loading for different structural models

Model	Beam ID	Location	Mmax (kN·m)	Vmax (kN)	Δ (mm)	AF_M	AF_V	AF_Δ
A (Control)	B 1	Axis (A-A)	52.64	82.67	0.94	1.00	1.00	1.00
	B 2	Axis (B-B)	45.94	80.16	0.97	1.00	1.00	1.00
	B 3	Axis (C-C)	42.16	78.50	1.02	1.00	1.00	1.00
F-1	B 1	Axis (A-A)	67.97	65.07	0.40	1.29	0.79	0.43
	B 2	Axis (B-B)	54.29	67.43	0.65	1.18	0.84	0.67
	B 3	Axis (C-C)	51.53	66.31	0.74	1.22	0.84	0.73
F-2	B 1	Axis (A-A)	111.25	93.15	0.96	2.11	1.13	1.02
	B 2	Axis (B-B)	42.90	74.45	0.87	0.93	0.93	0.90
	B 3	Axis (C-C)	39.80	72.74	0.90	0.94	0.93	0.88
F-3	B 1	Axis (A-A)	107.56	93.27	0.95	2.04	1.13	1.01
	B 2	Axis (B-B)	46.11	79.64	0.98	1.00	0.99	1.01
	B 3	Axis (C-C)	42.48	78.01	0.99	1.01	0.99	0.97
F-4	B 1	Axis (A-A)	99.85	88.67	0.85	1.90	1.07	0.90
	B 2	Axis (B-B)	45.77	79.37	0.96	1.00	0.99	0.99
	B 3	Axis (C-C)	42.48	78.01	0.99	1.01	0.99	0.97

Note: AF_Δ, AF_M, and AF_V represent the amplification factors of deflection, bending moment, and shear force, respectively, relative to the control model

In contrast, slab beams located on adjacent and remote axes (B2 and B3) exhibit only minor variations in bending moment demand, with AF_M values remaining close to unity (1.18–1.22 in model F-1 and approaching 1.00 as transfer beam depth increases), confirming that the influence of the transfer beam is highly localized and rapidly attenuates with increasing distance from the transfer axis. Shear force responses show comparatively limited sensitivity to changes in transfer beam dimensions, with a maximum shear amplification factor (AF_V) of approximately 1.13 observed for beam B1 in models F-2 and F-3, while beams B2 and B3 remain largely unaffected. Despite the amplification of internal force demands, slab beam deflections do not exhibit a corresponding increase, as reflected by AF_Δ values ranging between 0.43 and 1.02. This response highlights the effective role of the transfer beam in enhancing overall system stiffness and restraining serviceability-level deformations at the transfer floor [34]. These results are in line with previous analytical studies, which indicated that the influence of transfer beams on slab beams is highly localized and primarily governed by stiffness contrast and proximity to the transfer axis [35,36].

43.2 Deformation Behavior of Solid Slabs at the Transfer Level

According to ECP 203-2020 [23], the serviceability deflection limits for reinforced concrete solid slabs are governed by the general deflection criteria for beams and slabs, where the maximum final deflection, including the effects of creep and shrinkage, should not exceed L/240 of the clear span. For the 5.0 m span adopted in all solid slab models, this corresponds to an allowable deflection limit of approximately 20.8 mm. The deflection evaluation accounts for immediate, sustained, and long-term components to ensure an accurate representation of the service-life deformation behavior of the slab system.

As illustrated in Fig. 23, the control model (Model A) satisfies the serviceability requirement, exhibiting a maximum deflection of 19.20 mm, which remains below the allowable limit. In contrast, all models incorporating transfer beams exceed the permissible deflection. Model F-1 (40 × 50 cm) records the highest deflection of 30.93 mm, indicating a substantial serviceability violation. Increasing the depth of the transfer beam results in a progressive reduction in slab deflection to 26.36 mm, 24.48 mm, and 23.82 mm for Models F-2, F-3, and F-4, respectively. Despite this improvement, none of the transfer-beam configurations fully comply with the serviceability limit. This behavior highlights the significant impact of stiffness discontinuity and load concentration at the transfer level on slab deformation and underscores the necessity for stringent serviceability control in the design of transfer floor systems. This trend is also consistent with previous studies on transfer floors, which reported that stiffness discontinuity at the transfer level may amplify slab deformation and serviceability demand due to concentrated load transfer and slab–beam interaction effects [4,13].

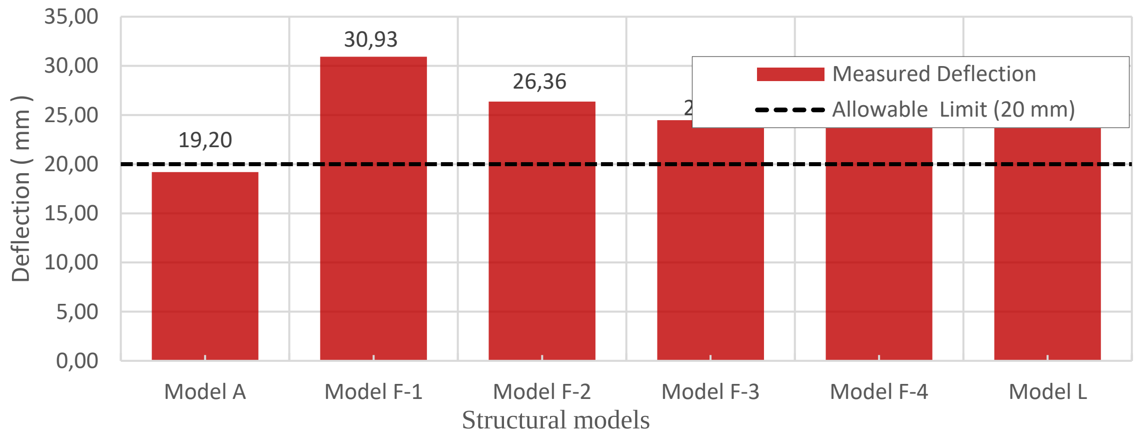

Fig. 23. Maximum deflection values for the slab in each structural model for group 1

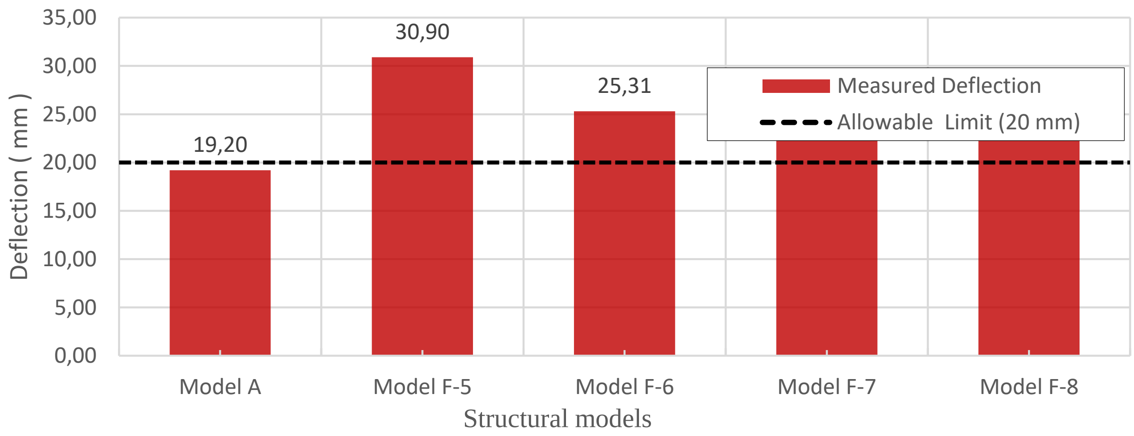

Fig. 24. Maximum deflection values for the slab in each structural model for group 2

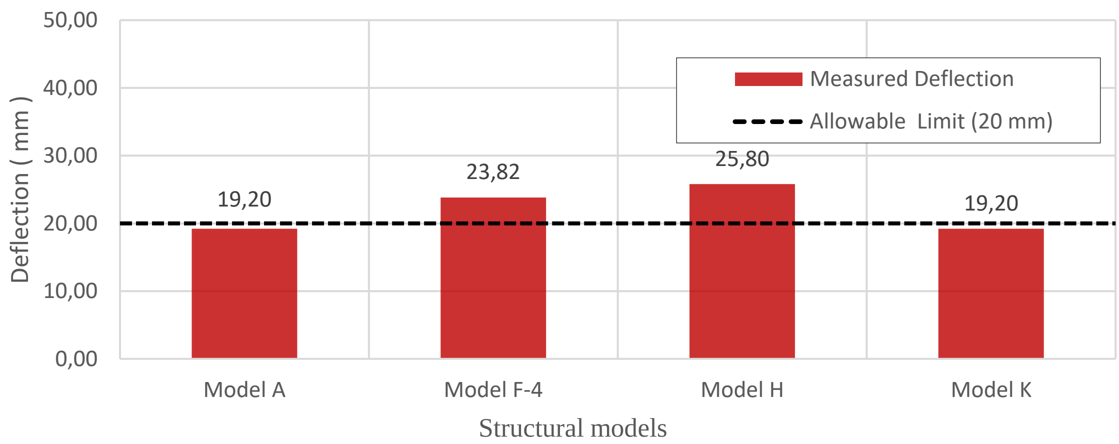

Fig. 25. Maximum deflection values for the slab in each structural model for group 3

For the solid slab system in Group 2, the control model (Model A) satisfies the ECP 203-2020 [18] serviceability requirement, exhibiting a maximum slab deflection of 19.20 mm, as shown in Fig. 24. The incorporation of continuous transfer beam configurations leads to an overall improvement in slab serviceability performance compared to simply supported systems; however, full compliance with the serviceability limit is not achieved. Model F-5 records the maximum deflection of 30.90 mm, corresponding to an increase of approximately 54.5% relative to the allowable limit. With increasing transfer beam stiffness and continuity, slab deflection is progressively reduced to 25.31 mm (+26.6%) in Model F-6, 23.01 mm (+15.1%) in Model F-7, and 22.66 mm (+13.3%) in Model F-8. A direct comparison with the corresponding simply supported configurations in Group 1 indicates that beam continuity provides a consistent, though moderate, reduction in slab deflection, which becomes more pronounced as transfer beam stiffness increases, achieving reductions of approximately 4.0–6.0%. The best continuous configuration (F-8) reduces deflection to 22.66 mm compared to 23.82 mm for the stiffest simply supported case (F-4), confirming that continuity enhances the effective stiffness and mitigates serviceability demands at transfer floors; nevertheless, the achieved improvement remains insufficient to fully satisfy the ECP 203-2020 [23] serviceability limit.

For the solid slab system in Group 3, the control model (Model A) satisfies the ECP 203-2020 [23] serviceability limit, exhibiting a maximum deflection of 19.20 mm, as shown in Fig. 25. The external placement of the transfer beam (Model F-4) increases slab deflection to 23.82 mm, representing a 24.06% increase relative to the control model. When the transfer beam is located internally (Model H), the slab experiences the highest deflection of 25.80 mm, corresponding to a 34.38% increase, which can be attributed to greater load concentration and reduced stiffness efficiency. In contrast, the centrally located transfer beam configuration (Model K) results in a deflection equal to that of the control model, indicating improved load balance and a more uniform stiffness distribution. These results demonstrate that the location of the transfer beam plays a critical role in governing slab deflection behavior and serviceability performance in solid slab systems.

4.4. Structural behavior of the building

4.4.1 Story displacement

Lateral displacement represents a key serviceability limit state in the design of multi-story buildings, particularly under wind and seismic actions. In this study, the maximum lateral displacements in both the X- and Y-directions were evaluated for the investigated models and compared with the reference control model (Model A), which does not include transfer beams or floating columns. Based on Fig. 27, Model A exhibits maximum displacements of 17.46 mm in the X-direction and 26.59 mm in the Y-direction. Upon introducing transfer beams with different cross-sectional dimensions (Models F-1 to F-4), the lateral response shows direction-dependent behavior. In the X-direction, a slight increase in displacement is observed, amounting to 1.89%, 1.78%, 2.86%, and 2.75% for Models F-1, F-2, F-3, and F-4, respectively. Conversely, the Y-direction exhibits modest displacement reductions of 7.22%, 5.00%, 3.65%, and 3.16%, respectively, indicating a limited improvement in lateral performance perpendicular to the transfer beam orientation.

In comparison, Model L, which incorporates a basement level, exhibits a pronounced increase in lateral displacement, reaching 14.61% in the X-direction and 9.86% in the Y-direction, as illustrated in Fig. 27. These results indicate that although transfer beams locally modify stiffness characteristics, their influence on the global lateral displacement response remains limited, as overall lateral stiffness is primarily governed by the shear wall system, which provides a continuous and efficient vertical load path for resisting wind and seismic actions [34,37]. The increased displacement observed in Model L is mainly attributed to altered dynamic characteristics and increased foundation flexibility, a behavior consistent with previous analytical and experimental studies showing that greater base flexibility can amplify roof-level displacements even in shear wall–dominated structures.

The influence of transfer beam continuity on lateral displacement was evaluated in Models F-5 to F-8 relative to the reference Model A*, as shown in Fig. 28. In the X-direction, the response shows limited sensitivity to continuity, where Model F-5 exhibits a slight increase in displacement by 1.37%, while Models F-6, F-7, and F-8 show small reductions of 0.86%, 4.41%, and 0.40%, respectively. In contrast, the Y-direction demonstrates more consistent improvements, with displacement reductions of 4.51%, 3.61%, 4.17%, and 1.58% for Models F-5 to F-8, respectively.

These results indicate that continuity provides modest but measurable displacement control, with the effectiveness depending on the dominant stiffness and load-resisting mechanisms governing each direction, as reflected by the directional variation observed in Fig. 28.

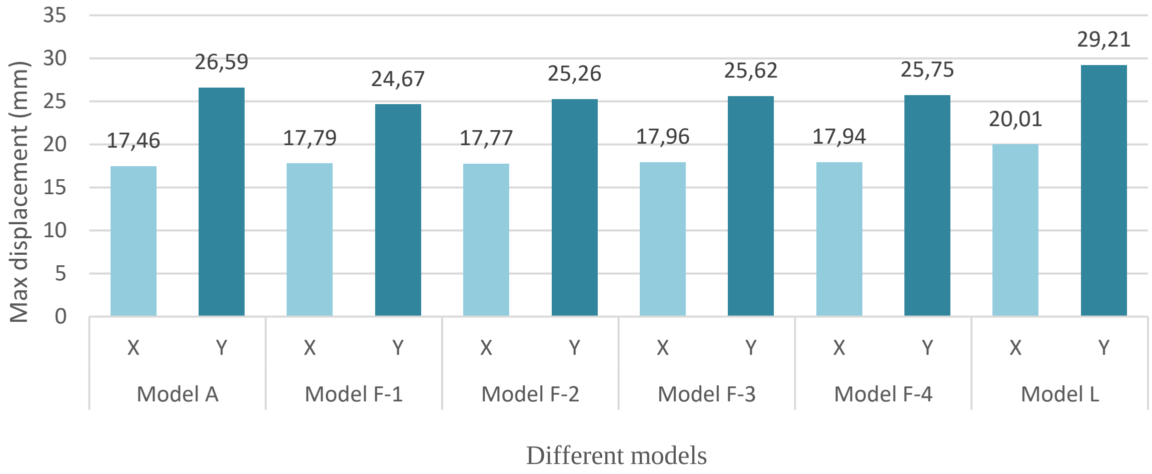

Fig. 27. Max displacement for models of group 1 (x-y) direction

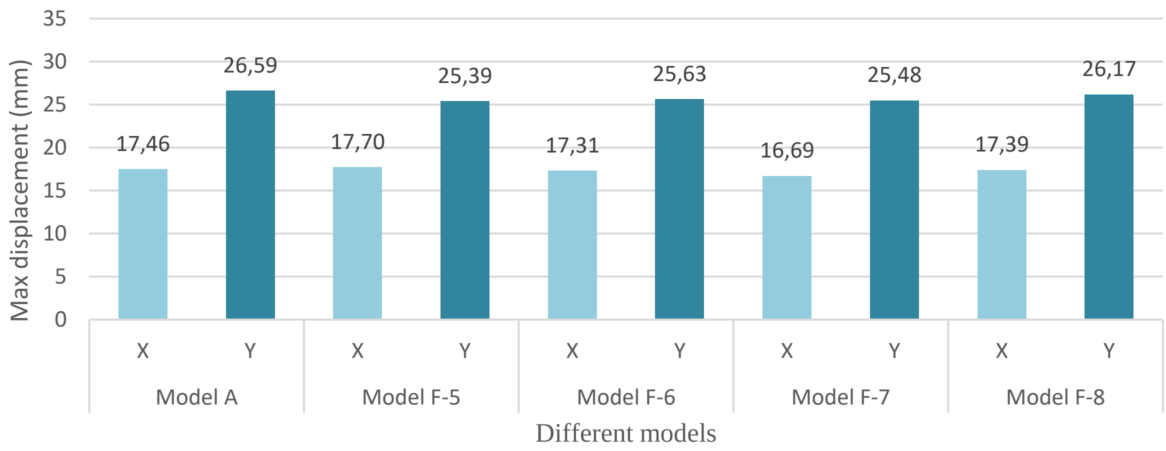

Fig. 28. Max displacement for models of group **2** (x-y) direction

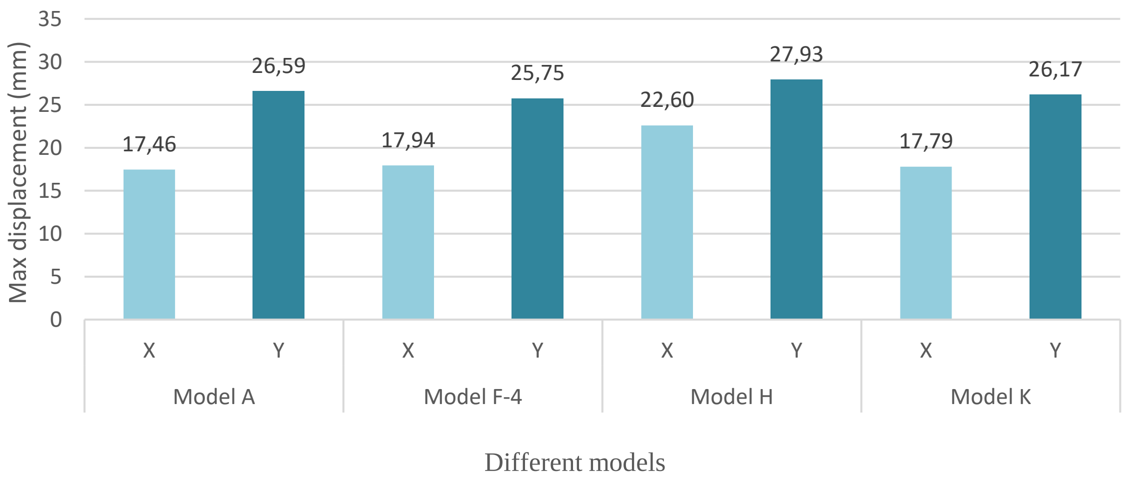

Fig. 29. Max displacement for models of group 3 (x-y) direction

The influence of transfer beam location on lateral displacement was assessed using Models F-4, H, and K, in which the transfer beam was shifted between external, intermediate, and central axes while maintaining the same cross-sectional dimensions. As shown in Fig. 29, relocating the transfer beam results in a direction-dependent response. Relative to the control Model A, Model F-4 exhibits a minor increase in X-direction displacement of 2.75% along with a 3.16% reduction in the Y-direction, while Model K shows similarly small variations (1.89% increase in X and 1.58% reduction in Y). In contrast, the intermediate placement (Model H) produces a pronounced amplification in lateral deformation, reaching 29.44% in the X-direction and 5.04% in the Y-direction, indicating a significant reduction in the effective global lateral stiffness and a change in the deformation pattern. Overall, these results demonstrate that transfer beam location may have a limited effect for peripheral and central configurations; however, certain locations—such as intermediate axes—can become critical by inducing unfavorable stiffness redistribution and substantially increasing lateral displacement. Therefore, transfer beam location should be considered alongside continuity and stiffness provisions when optimizing the lateral performance of structures incorporating transfer beam systems. The limited influence of transfer beam continuity and size on global displacement, compared with the more pronounced effect of unfavorable beam location, is in line with previous studies on vertically irregular buildings, where local transfer modifications had a secondary effect relative to the overall lateral load-resisting system [12,33,37].

4.4.2 Story Drift

Story drift, defined as the relative horizontal displacement between consecutive floors, represents a critical indicator of structural deformation under lateral loading. According to the Egyptian Code (ECP 203-2020) [23], the maximum allowable story drift is limited to 0.005h. For all examined models, the drift profiles exhibit a bell-shaped distribution, with peak values occurring between the 8th and 10th stories, reflecting the combined influence of mass and stiffness distribution along the building height, consistent with classical dynamic behavior Chopra, [26].

For Group 1 (Models F-1 to F-4 and L), increasing the transfer beam size leads to minor changes in story drift relative to the control Model A (Fig. 30). In the X-direction, drift values increase slightly from 1.84 mm in Model A to 1.88 mm, 1.88 mm, 1.90 mm, and 1.90 mm in Models F-1 to F-4, corresponding to increases of approximately 2.17%, 2.17%, 3.26%, and 3.26%, respectively. In the Y-direction, drift decreases from 2.82 mm in Model A to 2.63 mm, 2.69 mm, 2.72 mm, and 2.73 mm, representing reductions of 6.74%, 4.61%, 3.55%, and 3.19%, respectively. In contrast, Model L, which incorporates a basement, shows a more pronounced increase in drift, reaching 2.06 mm (X) and 3.00 mm (Y), equivalent to increases of 11.96% and 6.38%, respectively. This behavior is attributed to reduced base stiffness and altered deformation characteristics associated with the basement level.

For Group 2 (Models F-5 to F-8), introducing transfer beam continuity results in more noticeable drift reductions, particularly in the X-direction, as shown in Fig. 31. Relative to Model A, X-direction drift decreases from 1.84 mm to 1.87 mm, 1.84 mm, 1.77 mm, and 1.85 mm, corresponding to changes of +1.63%, 0.00%, −3.80%, and +0.54%, respectively. In the Y-direction, drift reduces from 2.82 mm to 2.70 mm, 2.72 mm, 2.69 mm, and 2.77 mm, reflecting reductions of 4.26%, 3.55%, 4.61%, and 1.77%, respectively. These results indicate that continuity provides a more effective mechanism for drift control than beam size alone, with a stronger influence along the axis aligned with the transfer beams.

For Group 3 (Models F-4, H, and K), varying the transfer beam location produces mixed effects on story drift, as illustrated in Fig. 32. Compared to Model A, Model F-4 exhibits an increase to 1.90 mm (X) and a reduction to 2.73 mm (Y), corresponding to +3.26% and −3.19%, respectively. Model K shows similar limited variations, with +2.17% in X and −1.77% in Y. In contrast, Model H demonstrates a substantial increase in drift, reaching 2.32 mm (X) and 2.93 mm (Y), equivalent to increases of 26.09% and 3.90%, respectively, indicating that intermediate beam placement can significantly reduce effective lateral stiffness and amplify deformation demands. Overall, the results confirm that transfer beam continuity provides the most effective reduction in story drift, followed by increasing beam size, while beam location generally has a secondary influence but may become critical for unfavorable configurations. Conversely, the inclusion of a basement consistently increases drift due to reduced base stiffness and modified dynamic response, in agreement with analytical observations reported for flexible-base structural systems. These observations are also consistent with previous analytical studies on buildings with floating columns and transfer systems, which showed that unfavorable irregularity configuration tends to increase drift demand, whereas improved continuity and stiffness distribution can mitigate inter-story deformation [11,12].

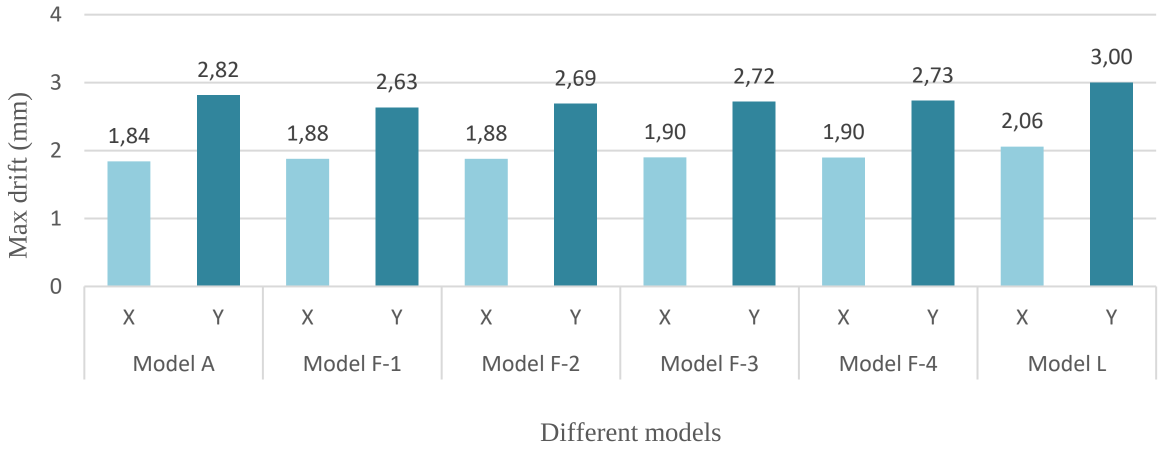

Fig. 30. Story drift curves for different models – group 1 – x-direction

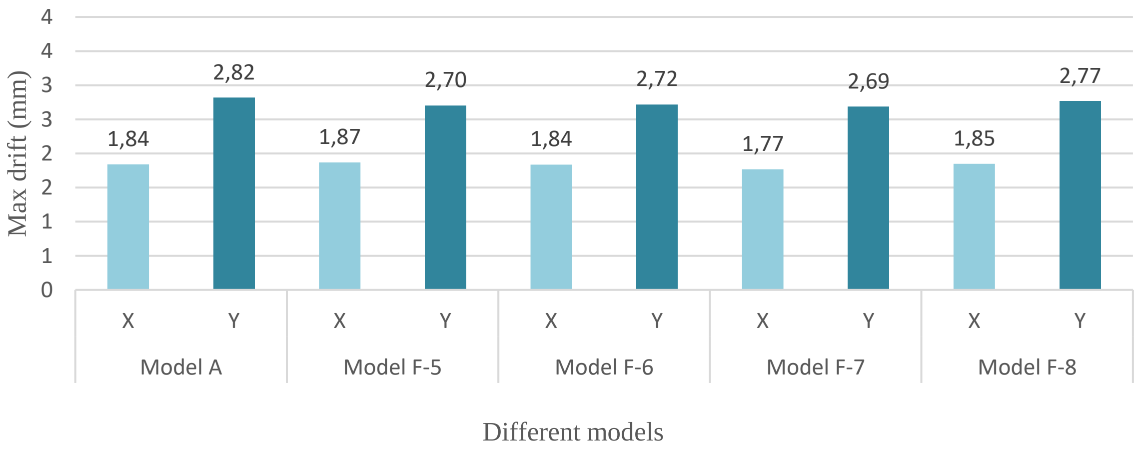

Fig. 31. Story drift curves for different models – group 1

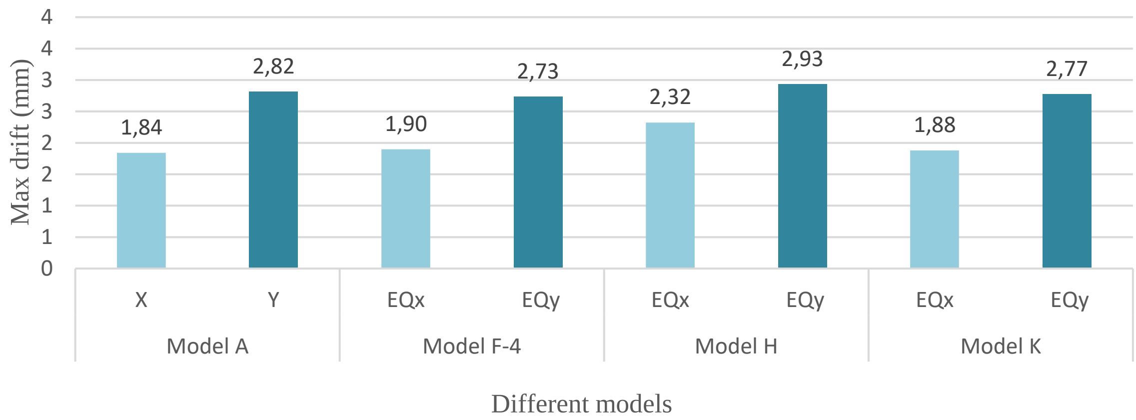

Fig. 32. Story drift curves for different models – group 3

4.4.3 Base Shear

The base shear values for the twelve structural models are identical in the X- and Y-directions, reflecting the symmetry of the lateral force–resisting system, while clear variations appear between the studied groups, as shown in Fig. 33.

In Group 1, increasing the transfer beam size (Models F-1 to F-4) leads to gradual increases in base shear from 1989.08 kN in Model A to 2004.38 kN, 2007.97 kN, 2006.20 kN, and 2007.30 kN, corresponding to increases of 0.77%, 0.95%, 0.86%, and 0.92%, respectively. In contrast, Model L, which includes a basement, shows a significant increase to 2203.75 kN (10.79%), attributed to added mass, increased effective height, and altered dynamic characteristics.

For Group 2, the introduction of transfer beam continuity (Models F-5 to F-8) results in moderate base shear changes of 0.70%, 1.26%, −2.15%, and 1.39%, respectively. While continuity generally increases stiffness and seismic participation, the reduction observed in Model F-7 reflects redistribution of internal forces rather than reduced seismic demand, consistent with findings by Abdelbaset et al., [1].

In Group 3, varying beam location produces limited but noticeable effects. Model H shows a reduction in base shear to 1880.94 kN (−5.45%), whereas Model K increases to 2012.47 kN (1.18%), indicating that central alignment enhances core participation and base shear demand. This trend aligns with the observations of Chopra, [26,34] regarding stiffness alignment and seismic force distribution.

These results are in agreement with established seismic behavior concepts, which indicate that base shear is primarily influenced by global mass and stiffness distribution, with transfer elements having a secondary effect unless significant irregularities are introduced [26].

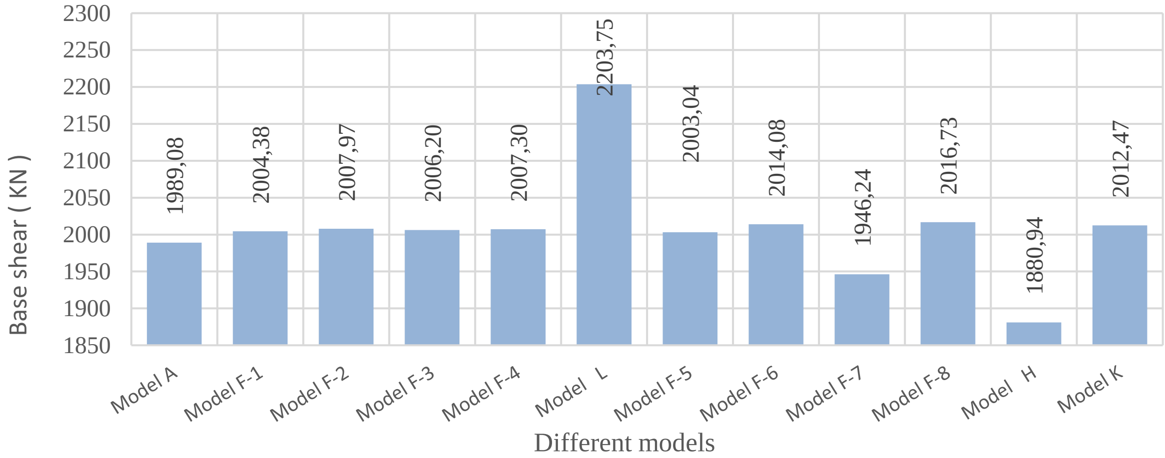

Fig. 33. Story base shear (x-y) direction for groups 1,2,3

5. Assumptions and Limitations of the Study

- The outcomes of this research should be interpreted in light of the modeling framework and analytical assumptions adopted herein. The structural response was evaluated using code-based linear elastic analysis procedures, including Equivalent Static Analysis (ESA) and Response Spectrum Analysis (RSA), in addition to Construction Stage Analysis (CSA) to simulate the effects of sequential construction. Accordingly, nonlinear material behavior was not explicitly incorporated, and both concrete and reinforcing steel were assumed to operate within the elastic domain. As a result, phenomena such as cracking, reinforcement yielding, stiffness degradation, and post-yield structural response were not captured in the present study.
- Time-dependent effects were partially considered through the implementation of CSA, which accounts for the progressive application of loads and the evolution of structural stiffness during construction. Nevertheless, creep and shrinkage were modeled using the

default constitutive formulations embedded in the analysis software, without calibration against experimentally measured material properties. While differential column shortening was inherently reflected through staged loading, it was not independently quantified or examined as a separate parameter.

- The scope of the study is primarily directed toward evaluating the global structural behavior and the performance of transfer beams. Key response parameters include bending moments, shear forces, deflections, axial load redistribution, story drift, and overall lateral displacements. However, localized phenomena such as punching shear at slab–column interfaces and other potential local failure mechanisms were not explicitly modeled. Consequently, the reported slab responses should be interpreted as indicators of global structural performance rather than as measures of localized capacity or failure.
- All numerical models correspond to a specific twelve-story reinforced concrete building, with one configuration including a basement level, designed in accordance with the Egyptian Code provisions. Although the investigated configurations and parametric variations reflect commonly encountered design scenarios, the applicability of the results is inherently limited to structures with similar geometric characteristics, structural systems, and seismic design conditions.
- Notwithstanding these limitations, the adopted analytical framework offers a consistent and systematic basis for comparative evaluation. It enables a reliable assessment of the relative influence of transfer beam characteristics, slab system interaction, and construction sequencing on both seismic response and serviceability performance.

6. Conclusions

- Construction Stage Analysis CSA proved the most reliable approach for transfer beam assessment, producing up to 34.77% higher bending moments, 28.85% higher shear forces, and 5.70% higher deflections than RSA, while exceeding ESA by 35.54%, 25.35%, and 57.72%, respectively. By explicitly capturing staged loading, creep, shrinkage, and time-dependent load redistribution, CSA delivers the most conservative and realistic representation of transfer beam behavior under actual construction conditions.
- Increasing transfer beam depth from 400×500 mm to 800×1600 mm reduced mid-span deflections by up to 82.79% under CSA but increased bending moments and shear forces by 398.79% and 247.80%, respectively, due to stiffness-driven load redistribution. Only the shallowest sections (400×500 mm) failed the international deflection limit of L/500, while deeper configurations satisfied serviceability requirements, confirming that adequate transfer beam proportioning is essential for long-term performance under construction-stage conditions.
- Under the Egyptian Code L/250 serviceability criterion, most transfer beam configurations increased slab deflection compared to the control model (19.20 mm). The shallowest section (400×500 mm) produced the highest deflection of 30.93 mm (+61.1%), while progressive depth increases to 800×1000 mm, 800×1400 mm, and 800×1600 mm reduced deflections to 26.36 mm, 24.48 mm, and 23.82 mm, respectively, though all exceeded the allowable limit.
- Beam continuity further improved performance, with the stiffest continuous configuration (800×1600 mm) achieving 22.66 mm (+13.3% exceedance). Only the centrally located transfer beam configuration restored slab deflection to the control level, fully satisfying the L/250 requirement and confirming that beam continuity and favorable positioning are critical for controlling slab serviceability.
- Continuous transfer beams integrated with solid slabs provided improved internal action redistribution compared to simply supported configurations. Under CSA, continuity reduced mid-span deflections by 9.79% to 17.36% for stiffer sections (800×1000 mm to 800×1600 mm), while the shallowest section (400×500 mm) showed negligible change (+0.27%). Flexural demands decreased by up to 14.10% due to enhanced moment redistribution, while shear forces increased marginally (0.40% to 2.65%) from continuous load paths. Overall, continuity enhances structural integration and

serviceability—particularly for stiffer configurations—while introducing slight shear increases that require design consideration.

- Transfer beam location critically governs structural demand distribution in solid slab systems with floating columns. Peripheral placement reduced floating column axial force by 41.3%, proving most effective for load redistribution. Intermediate placement increased axial demand by 16.6%, indicating unfavorable stiffness compatibility, while central placement nearly restored original axial forces (0.14% reduction) but concentrated demands in the building core, increasing bending moments by 16.4% and shear forces by 29.0% compared to peripheral configuration. These results confirm that peripheral placement promotes efficient load dispersion and improved structural performance, while central placement concentrates gravity and seismic demands in core columns, emphasizing the critical importance of transfer beam location in solid slab system design.
- Axial load redistribution in floating-column systems follows a stiffness-proportional mechanism. Removing the ground-floor column reduced floating column axial loads by 86.9% for the smallest section (400×500 mm) to 41.3% for the deepest (800×1600 mm). Basement inclusion significantly altered this behavior, showing 50.3% reduction despite using the same deep section, indicating modified global stiffness. Directly connected columns experienced load amplification up to 47.7% in standard configurations, increasing to 61.9% with basement inclusion due to enhanced alternative load path participation. These findings confirm that transfer beam geometry, stiffness, and basement presence collectively govern axial load redistribution in vertically discontinuous structures.
- Transfer beam presence has limited influence on global lateral displacement and base shear, with effects more pronounced in inter-story drift and unfavorable configurations. Varying transfer beam sizes produced minor displacement changes (up to +2.86% in X-direction and −7.22% in Y-direction), confirming that shear walls primarily govern global stiffness. Beam continuity provided modest displacement reductions up to 4.51%. However, unfavorable beam location—particularly intermediate placement—significantly amplified lateral deformation by up to 29.44%. Drift profiles showed bell-shaped distribution with peaks between the 8th and 10th stories, consistent with classical structural dynamics. Base shear variations remained limited for beam size (0.77%–0.95%) and continuity (−2.15% to +1.39%), while intermediate beam location reduced base shear by 5.45%, and basement inclusion increased it by 10.79%, highlighting sensitivity to base flexibility and altered dynamic characteristics.
- CSA consistently provides higher and more realistic structural demands than ESA and RSA, as it accounts for construction sequencing, creep, shrinkage, and long-term load redistribution, making it essential for accurate serviceability assessment and compliance with ECP 203-2020 [18].
- The parametric investigation confirms that the performance of transfer beam systems is controlled by the combined effects of beam geometry, continuity, and in-plan location. Configurations employing larger, continuous transfer beams positioned along the building perimeter provide the most efficient structural response, achieving a balanced reduction in axial force demands, improved slab stress distribution, and effective control of deflections under both gravity and seismic loading conditions.
- Collectively, the findings of this study demonstrate that the seismic behavior of reinforced concrete solid slab structures incorporating transfer beam systems is governed by the combined effects of beam geometry, continuity, in-plan location, and construction sequencing. The present work makes a novel contribution by providing the first integrated ESA, RSA, and CSA framework specifically applied to solid slab buildings with floating columns, offering quantitative design-oriented insights not previously available in the literature. The results confirm that Construction Stage Analysis is essential for realistic assessment of transfer beam systems, and that peripheral placement of continuous, deep transfer beams provides the most efficient structural configuration

under combined gravity and seismic loading. These findings provide practical guidance for structural engineers designing buildings with transfer floor systems in seismic regions.

6.1 Recommendations

- Mandate Construction Stage Analysis (CSA) for transfer beam design in buildings with floating columns to capture time-dependent effects and realistic structural demands.
- Revise the Egyptian Code ECP 203-2020 [18] to introduce explicit serviceability limits for transfer beams, recommending a deflection limit of L/500 or stricter, in alignment with ACI 318, BS 8110, Eurocode 2, and AS 3600, particularly for long-span transfer floors.
- Mandate minimum transfer beam dimensions of 800×1400 mm for solid slab systems and prioritize continuous configurations to ensure adequate serviceability and force redistribution.
- Prioritize peripheral transfer beam placement to minimize structural demands. Avoid intermediate and central placements unless architecturally essential and supported by enhanced stiffness and detailing.
- Consider transfer beam–slab interaction explicitly in design, ensuring adequate compatibility between slab stiffness and transfer beam rigidity to prevent excessive deformation and stress concentration at transfer levels.

Nomenclature

- SMRF : Special Moment Resisting Frame.
- C_t^R : the natural period coefficient for structures dominated by shear walls.
- T^S, T^R: the approximate fundamental period of the structure based on its total height H (in meters).
- C_U: the upper bound modification coefficient used to limit the natural period used in design According to ECP-203, this coefficient is used to set an upper limit for the estimated period, especially to avoid unconservative values in tall or irregular buildings.
- T_U^R: the modified approximate period after applying the upper limit factor. It is used in some cases to calibrate the period used in the seismic design.
- T^M: the first-mode natural period, which is directly obtained from modal analysis using software ETABS.
- T^R: the final period used in design calculations. The smaller value between the modified empirical period and the modal period is adopted to ensure conservative seismic force estimation.
- T^M is obtained automatically from modal analysis but T^R is either entered manually or calculated externally, the minimum between T^M and T_U^R is then used to define the design base shear, ensuring code-compliant and safe results.
- VRSA, VESA: the base shear forces calculated from ESA, RSA.
- D.L: Dead Load
- L.L: live load
- α: A superposition factor that takes into account the effect of the main semi-permanent live loads on top of the structure during an earthquake.
- EQ(x, y): Static seismic force in x and y directions, respectively.
- ecc: Eccentricity, which is imposed with a value of 0.05.
- R.SX, Y, Z: response spectrum seismic force in x, y, and z direction, respectively.
- T.B: means transfer beam.

References

[1] Abdlebasset YM, Sayed-Ahmed EY, Mourad SA. Seismic analysis of high-rise buildings with transfer slabs: State-of-the-art review. Electronic Journal of Structural Engineering. 2016;16(1):38-54. https://doi.org/10.56748/ejse.16209
[2] El-Mahdy OO, Refat HM, Abd El-Salam AM, El-Bayome ESZ. Towards seismic performance of tall buildings with transfer floors. Engineering Research Journal. 2022;51:56-72. https://doi.org/10.21608/erjsh.2022.224292
[3] Taranath BS. Structural analysis and design of tall buildings. CRC Press; 2016. https://doi.org/10.1201/b11248

[4] El-Bayome ESZ, Abd El-Salam AM, El-Mahdy OO, Refaat HM. Seismic assessment of high-rise buildings having transfer elements. Electronic Journal of Structural Engineering. 2023;23(4):14-24. https://doi.org/10.56748/ejse.23433
[5] Işık E, Shao YB, Hadzima-Nyarko M, Radu D, Bulajic B, Lozancic S. Enhancing the seismic safety of upgraded RC buildings using FRP retrofitting: analytical and field evidence from the 2023 Kahramanmaraş earthquakes. Bulletin of Earthquake Engineering. 2026;24:1467-1501. https://doi.org/10.1007/s10518-025-02338-z
[6] Yuzbasi J. Post-earthquake damage assessment: Field observations and recent developments with recommendations from the Kahramanmaraş earthquakes in Türkiye on February 6th, 2023 (Pazarcık M7.8 and Elbistan M7.6). Journal of Earthquake Engineering. 2025;29(16):3367-3392. https://doi.org/10.1080/13632469.2024.2353864
[7] American Concrete Institute. ACI 318-19: Building code requirements for structural concrete and commentary. American Concrete Institute; 2019.
[8] Abbood IS. Strut-and-tie model and its applications in reinforced concrete deep beams: A comprehensive review. Case Studies in Construction Materials. 2023;19:e02643. https://doi.org/10.1016/j.cscm.2023.e02643
[9] Ismail KS, Guadagnini M, Pilakoutas K. Strut-and-tie modeling of reinforced concrete deep beams. Journal of Structural Engineering. 2018;144(2). https://doi.org/10.1061/(ASCE)ST.1943-541X.0001974
[10] Sumathi VR, Vijayan S. Comparative study on rebar and post-tensioned transfer girder. International Journal of Engineering Research & Technology (ICONNECT 2022). 2022;10(9).
[11] Bashir AA, Mohammed KS, Kambal MEM. Performance study of floating columns subjected to vertical loads. Journal of Karary University for Engineering and Science. 2024;2(2).
[12] Gajbhiye A, Aswin CP. Effect of floating column locations in RC multistorey building with shear wall subjected to seismic load. International Journal for Scientific Research & Development. 2021;9(3):82-86. https://doi.org/10.22214/ijraset.2021.38011
[13] Elawady AK, Okail HO, Abdelrahman AA, Sayed-Ahmed EY. Seismic behaviour of high-rise buildings with transfer floors. Electronic Journal of Structural Engineering. 2014;14(2):57-70. https://doi.org/10.56748/ejse.14181
[14] Mutalikdesai T, Kapali K. Study and comparison of conventional analysis with construction sequence analysis using ETABS. International Journal of Engineering Research & Technology. 2022;11(9).
[15] Elansary AA, Metwally MI, El-Attar A. Staged construction analysis of reinforced concrete buildings with different lateral load resisting systems. Engineering Structures. 2021;242:112535. https://doi.org/10.1016/j.engstruct.2021.112535
[16] Ha T, Kim S. Prediction of time-dependent lateral movement induced by differential shortening in tall buildings using construction stage analysis. International Journal of High-Rise Buildings. 2017;6(1):11-19. https://doi.org/10.21022/IJHRB.2017.6.1.11
[17] Sadouki A, Djafar-Henni I. Structural response of transfer beams: Evaluating the effect of staged construction. International Journal of Advanced Natural Sciences and Engineering Researches. 2024;8(9):55-63.
[18] Mitra A, Aditya L, Parthe V, Tamizharasi G, Senthilkumar R. Assessing earthquake resilience in RC buildings: The role of transfer beams and trusses on structural integrity. Structures. 2024;70:107885. https://doi.org/10.1016/j.istruc.2024.107885
[19] Thant NN, Kyaw TY. Study on the effect of response spectrum analysis and construction sequence analysis on setback steel structure. International Journal of Trend in Scientific Research and Development. 2019;3(4):1349-1355.
[20] Housing and Building National Research Center. Egyptian Code for Loads and Forces (ECP 201:2012). Ministry of Housing, Utilities and Urban Communities, Cairo, Egypt; 2012.
[21] El-Kholy AM, Sayed H, Shaheen AA. Comparison of Egyptian Code 2012 with Eurocode 8-2013, IBC 2015 and UBC 1997 for seismic analysis of residential shear-wall RC buildings in Egypt. Ain Shams Engineering Journal. 2018;9(4):3425-3436. https://doi.org/10.1016/j.asej.2018.07.004
[22] Computers and Structures, Inc. ETABS user's guide. Computers and Structures, Inc.; 2022.
[23] Egyptian Code Committee. ECP 203-2020: Design and construction of reinforced concrete structures. Ministry of Housing, Utilities and Urban Communities, Cairo, Egypt; 2020.
[24] El-Mahdy OO, Refat HM, Abd El-Salam AM, El-Bayome EZ. Towards seismic performance of tall buildings with transfer floors. Engineering Research Journal (ERJ). 2022;1(51):56-72. https://doi.org/10.21608/erjsh.2022.224292
[25] Durabi K, Sunkari S. Inelastic seismic behavior of floating column building considering soil-structure interaction. In: Pathak KK, Singla R, Bhardwaj S, Kundu A, editors. Latest developments in civil engineering (Vol. 352). Springer; 2024. p. 55-61.
[26] Chopra AK. Dynamics of structures: Theory and applications to earthquake engineering. 5th ed. Pearson; 2017.

[27] British Standards Institution. BS 8110-1:1997: Structural use of concrete - Part 1: Code of practice for design and construction. BSI; 1997.
[28] European Committee for Standardization. EN 1992-1-1: Eurocode 2: Design of concrete structures - Part 1-1. CEN; 2004.
[29] Standards Australia. AS 3600:2018 - Concrete structures. Standards Australia; 2018.
[30] Izzuddin BA, Vlassis AG, Elghazouli AY, Nethercot DA. Progressive collapse of multi-storey buildings due to sudden column loss: Part I. Engineering Structures. 2008;30(5):1308-1318. https://doi.org/10.1016/j.engstruct.2007.07.011
[31] Structure Magazine. Stiffness versus strength. Structure Magazine; 2015.
[32] Lingampally KC, Veerupakshi S. Definitive positioning of floating columns in multistory buildings using ETABS. AIP Conference Proceedings. 2024;3146(1):060008. https://doi.org/10.1063/5.0224708
[33] Saleh MSM, Tawfic YR, Abd Hafez LM, Fahmy NG. Seismic response of reinforced concrete flat slab structures with transfer beams subjected to lateral loads. Journal of Engineering Sciences (JES). 2026;53(601), Special Issue: ICCE2025. https://doi.org/10.21608/jesaun.2026.441584.1858
[34] Londhe RS. Studies in transfer beams for high-rise buildings [Doctoral dissertation]. Indian Institute of Technology Roorkee; 2007.
[35] Londhe RS. Shear strength analysis and prediction of reinforced concrete transfer beams in high-rise buildings. Structural Engineering and Mechanics. 2011;37(1):39-59. https://doi.org/10.12989/sem.2011.37.1.039
[36] Saleh MSM, Tawfic YR, Abdel-Hafez LM, Fahmy NG. Structural and seismic behavior of transfer beam systems in flat slab and solid slab buildings: A comparative study using ESA, RSA, and CSA. SVU-International Journal of Engineering Sciences and Applications. 2026;7(1):187-230. https://doi.org/10.21608/svusrc.2026.465859.1321
[37] Islam MM, Mofiz SA. Effect of positioning of shear walls in a multi-storied building on response to earthquake. Engineering Research Express. 2024;6(2). https://doi.org/10.1088/2631-8695/ad43b8